PE&RS

October 2023 Volume 89, Number 10

PHOTOGRAMMETRIC ENGINEERING & REMOTE SENSING

The official journal for imaging and geospatial information science and technology

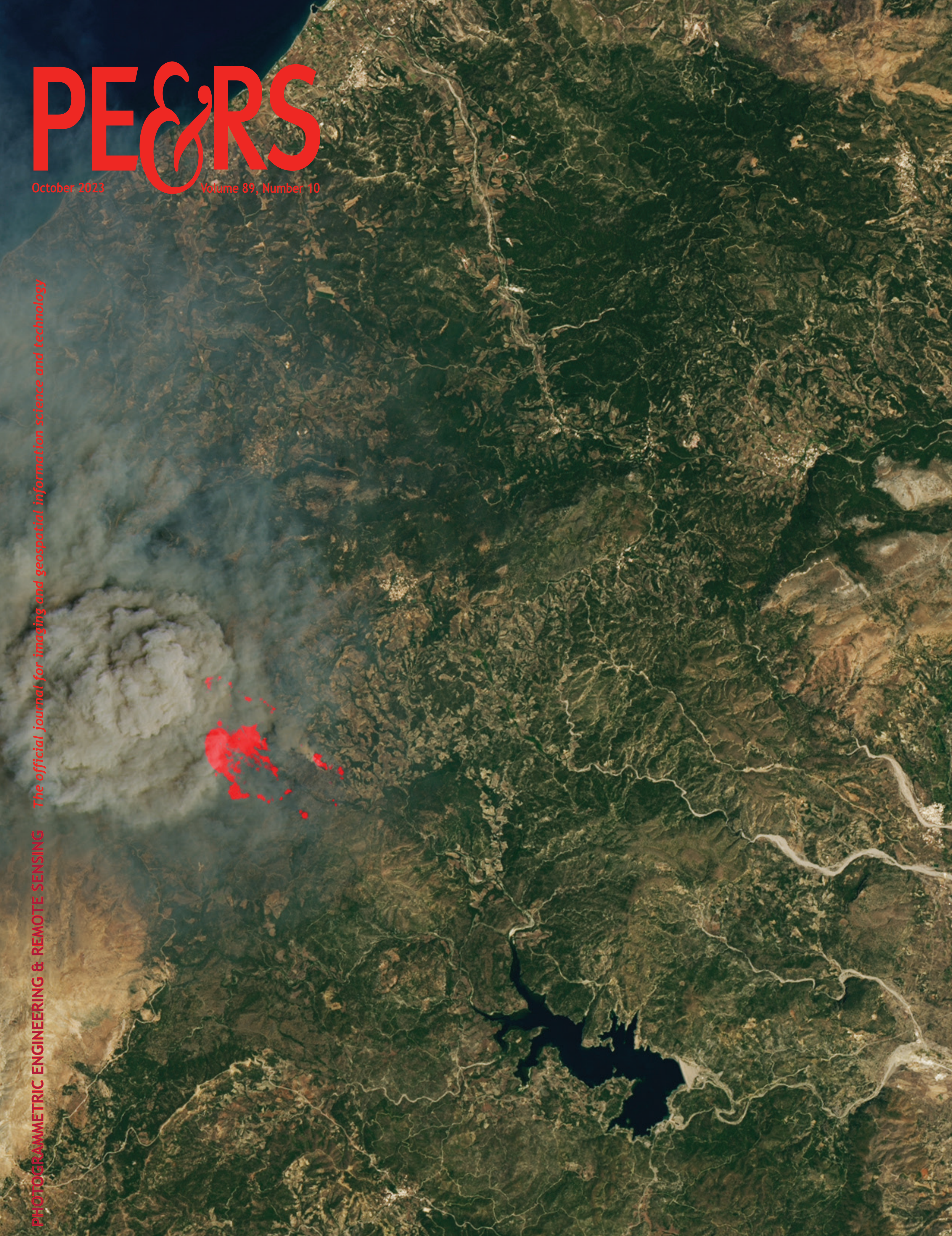

To have your press release published in *PE&RS*, contact Rae Kelley, rkelley@asprs.org.

ANNOUNCEMENTS

TCarta Marine, a global provider of hydrospatial products and services, has been awarded a contract to deliver satellite derived bathymetry (SDB) and seafloor classification data for the coastal zones of 13 regions around the world to the National Geospatial-Intelligence Agency (NGA) under contract to Maxar Technologies.

TCarta will deliver seabed depth and feature maps from high-resolution multispectral Maxar WorldView-2 and WorldView-3 satellite imagery for the 13 regions. SDB measurements are accurate to depths of 20-30 meters depending on water conditions, with two-meter spatial resolution. Feature classification includes coral reefs, large rocks, sandbars, and other navigation hazards.

TCarta has processed thousands of Maxar satellite images for the project, including hundreds of high-resolution scenes for one nation alone. By the time all deliverables have been submitted and approved by NGA, TCarta will have mapped the entire subsurface coastlines of the 13 regions over the 12-month Period of Performance.

"This is the most ambitious SDB mapping program ever conducted in terms of both geographic area and timeline," said TCarta President Kyle Goodrich. "In particular, one 7,239-square-kilometer coastline by itself is larger than any contiguous SDB project TCarta has undertaken."

"SDB can be particularly useful for remote or hard-to-access locations and for areas where traditional survey methods are too expensive or time consuming," said Jennifer Krischer, Maxar's Vice President and General Manager, Intelligence Programs. "The partnership between Maxar and TCarta offers a valuable service to NGA for accurate and efficient bathymetric data collection, which reflects NGA's renewed emphasis on collecting data and generating insight 'from Seabed to Space'."

A leader in the application of SDB technology worldwide for more than a decade, TCarta has played a key role in enhancing the traditional water depth extraction methodology. With funding from Small Business Innovation Research (SBIR) programs managed by NOAA and the National Science Foundation, the Denver firm has integrated machine learning algorithms into the processing workflow and introduced the use of space-based laser data from the NASA ICESat-2 satellite to validate SDB results.

"A major challenge with this project was the variety of turbid and silty water conditions encountered in different geographic regions, but NGA has been receptive about the results," said Goodrich. "We have bolstered and refined our existing workflows to deliver products that meet NGA requirements."

CompassCom Software has released Version 8.2 of the CompassCom GIS-centric hybrid telematics platform that can be deployed on premises or in the cloud for real-time asset tracking and comprehensive fleet management. The new version offers enhanced ease of use and more robust analytics and reporting functionality for safer, more efficient and secure fleet operations.

Developed on Esri ArcGIS technology and now supporting JavaScript 4.0, the CompassCom telematics software platform is used worldwide to track the real-time locations and status of personnel, vehicles, and other mobile assets. The platform is relied upon by critical infrastructure work forces – including public works and public safety offices – as well as departments of transportation and national government security agencies.

"Building on our 29 years as an Esri Business Partner, we have leveraged the full range of GIS capabilities in Version 8.2 to deliver superior situational awareness related to the safety of personnel and efficient operations of vehicles," said CompassCom CEO Brant Howard. "Customized alerts and dashboards provide fleet managers with the information they need to make better decisions in real time."

The flexible CompassCom telematics platform receives location and status data from any GPS-equipped vehicle, handheld device, or high-value asset and serves that information in real-time to a GIS map display or an interactive dashboard. Live alerts give managers instant insight into fleet activities for better decision making, while real-time vehicle performance analytics and reporting enable fine tuning of operational efficiencies.

CompassCom developed the telematics solution to utilize Esri JavaScript API and Esri data formats, The platform also offers data portability to CAD systems, asset management, and other third-party GIS environments. When the client or agency requires hardened secure installations CompassCom offers on premises behind a firewall on the customer's private network as an option.

"The CompassCom telematics platform is now easier to use and runs exactly the same in the cloud or on premise," said Howard.

For more information on the CompassCom V8.2 telematics platform or to schedule an online demonstration, visit the CompassCom website at www.compasscom.com.

Bowman Consulting Group Ltd. (the "Company" or "Bowman") (NASDAQ: BWMN), today announced the acquisition of MTX Surveying, Inc. ("MTX"), a geospatial, land survey and project management company based in Marshall, Texas. Founded by Shane Nafe and Austin Holland in 2016, the firm has grown rapidly to a workforce of over 60 accredited professionals, technicians, and support staff serving clients in Texas, Louisiana, and New Mexico. Today, MTX provides full-service consulting, project management, surveying, mapping, and permitting services for clients working in oil and gas, energy and renewables, utility services, and land development. The MTX staff will all become Bowman employees in connection with the acquisition.

"Shane and Austin have built an exciting company," said Gary Bowman, CEO of Bowman. "Their focus on oil and gas, energy, and renewables projects will help to accelerate our goal of increasing the contribution of power and utility-oriented assignments within our revenue mix. Their experience with aerial mapping, data capture, hi-res orthometric imagery, and drone surveying complements other recent acquisitions and investments we have made in geospatial technologies and services."

"We're pleased to be joining Bowman and are excited about the opportunities this acquisition provides," said Shane Nafe, President and Founding Partner of MTX Surveying. "Bowman has an expansive national platform of clients, assignments, and engineering professionals to which we can contribute immediately. We're ready to get started adding value and growing our collective energy services and geospatial practice."

For more information on MTX Surveying, their projects, and services, visit https://www.mtxsurveying.com.

EVENTS

GoGeomatics Launches Canada's Inaugural Geospatial Exposition in Calgary—Canada's geospatial community is coming together for the first-ever national geospatial exposition in Calgary. The GoGeomatics Expo will take place November 6-8th on the iconic Calgary Stampede grounds.

Co-located with the Expo, the GeoIgnite Career Fair is where Canada's top organizations will recruit from a diverse pool of professionals, including students and graduates from the Expo's Education Partners, the University of Calgary Geomatics Engineering Program and the SAIT Geomatics Program.

The GoGeomatics Expo fosters collaboration and will showcase the latest advancements in the geospatial sector. This community-driven event provides an arena for professionals to connect, share ideas and stay updated on the latest developments in research, technologies and services. The event will feature an array of engaging activities, including keynote presentations, panel discussions, workshops and interactive exhibitions.

Highlights of the GoGeomatics Expo include:

- Speaking Programs: Renowned experts in the geospatial field will be sharing insights on industry trends, challenges and future opportunities. Thought-provoking panel discussions will bring together experts from various sectors to explore how geospatial technology is shaping industries across Canada. Themes of discussions are: reality capture, earth observation, BIM/GIS, surveying, leadership, education and public good (government).
- Activities: The trade show will feature cutting-edge geospatial products, solutions and services from engineering firms, product and software developers, navigation specialists, satellite experts and more. Demos and workshops will allow participants to enhance their skills and knowledge in geospatial tools, data analysis and geographic information systems (GIS). The SCAN-Off is a friendly opportunity for companies to participate in a scan-to-scan comparison of their LiDAR mapping platforms.
- Networking Opportunities: The GoGeomatics Expo will provide ample opportunities for attendees to network with other professionals, potential employers and industry influencers. From a networking zone on the trade show floor, to the Expo party and the ticketed opening reception and dinner, everyone will have the chance to connect.

"The Expo is about bringing the geospatial and geomatics communities together to learn, network and exchange ideas," says GoGeomatics founder and Managing Director, Jonathan Murphy. "Everyone is welcomed to this celebration of our sector."

Registration for the GoGeomatics Expo is now open. For more information about the event please visit the official GoGeomatics Expo website at: www.gogeomaticsexpo.com.

CALENDAR

- 16-19 October, **GIS-Pro 2023**, Columbus, Ohio; www.urisa.org/gis-pro.
- 30 October - 3 November, ACRS2023, Taipei, Taiwan; https://acrs2023.tw.
- 6-8 November, **GoGeomatics Expo**, Calgary, Alberta, Canada; https://gogeomaticsexpo.com.
- 8-10 November, **Smart GEO Expo 2023**, Seoul, South Korea; https://smartgeoexpo.kr.
- 27 November - 1 December, **URISA GIS Leadership Academy**, Denver, Colorado; https://urisa-portal.org/page/URISA_GLA.
- 11-13, February 2024, **Geo Week**, Denver, Colorado; https://www.geo-week.com.
- 2-4 May, **GISTAM 2024**, Angers, France; https://gistam.scitevents.org.
- 13-16 May 2024, **Geospatial World Forum**, Rotterdam, The Netherlands; https://geospatialworldforum.org.

PE&RS
PHOTOGRAMMETRIC ENGINEERING & REMOTE SENSING
The official journal for imaging and geospatial information science and technology
October 2023 Volume 89 Number 10

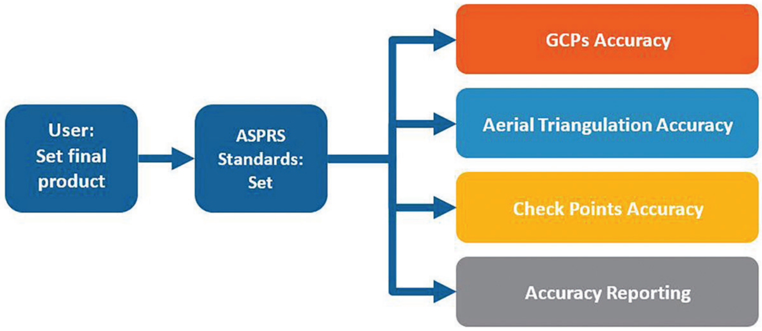

COLUMNS

ANNOUNCEMENTS

DEPARTMENTS

Lotus wetland is a type of wetland that can efficiently purify water. Therefore, rapid and accurate remote sensing monitoring of the distribution of lotus wetland has great significance to their conservation and the promotion of a sustainable and healthy development of ecosystems. The phenology-based method has proven effective in mapping some different types of wetlands. However, because of the serious absence of remote sensing data caused by cloud coverage and the differences in the phenological rhythms of lotus wetlands in different areas, achieving high-precision mapping of different regions using a unified approach is a challenge. To address the issue, this article proposes a Phenology Normalized Lotus Index (PNLI) model that combines SAR time-series imagery and the phenology-based method.

Many remote sensing and geoscience applications require a high-precision terrain model. In 2022, the Forest And Buildings removed Copernicus digital elevation model (FABDEM) was released, in which trees and buildings were removed at a 30 m resolution. This research aims to perform a qualitative and quantitative analysis of FABDEM in comparison with the commonly used global DEMS.

Surface reconstruction has been studied thoroughly, but very little work has been done to address its evaluation. In this article, we propose new visibility-based metrics to assess the completeness and accuracy of three-dimensional meshes based on a point cloud of higher accuracy than the one from which the reconstruction has been computed.

Urban vegetation phenology is important for understanding the relationship between human activities on urban ecosystems and carbon cycle. The relationship between urban and rural vegetation phenology and environmental and meteorological factors were studied across urban-rural gradients. However, the relationship of intra-urban urbanization intensity (UI) gradients on vegetation at the start of season (SOS) is unclear. Here, we used remote sensing data to quantitatively assess the relationship of vegetation SOS to UI gradients at mid-high latitudes in the northern hemisphere.

See the Cover Description on Page 580

COVER DESCRIPTION

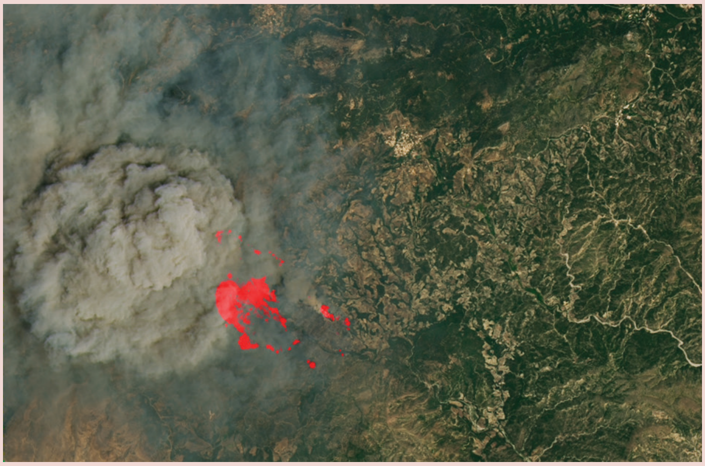

Wildfires raging across the Greek island of Rhodes sent tens of thousands of locals and tourists scrambling for safety in late July 2023. A prolonged stretch of extreme heat contributed to high fire risk across much of the country. Blazes also ignited on the mainland and the islands of Corfu and Evia.

The Operational Land Imager (OLI) on Landsat 8 acquired this image of fire activity on Rhodes on July 19. The image is natural color, with the infrared signature from actively burning fires overlaid in red. Thick smoke can be seen drifting westward toward the Aegean Sea.

This image captures the start of what turned into an intense period of wildfire. NASA-affiliated scientists were able to track the fires' spread with the Visible Infrared Imaging Radiometer Suite (VIIRS) sensor on the NASA-NOAA Suomi NPP satellite. Calculating the perimeter of actively burning areas every 12 hours, Eli Orland and Tess McCabe observed how the Rhodes fire spread relatively slowly at first, then picked up rapidly. Between July 21 and July 23, it underwent a six-fold increase in size, from approximately 25 to 150 square kilometers (10 to 60 square miles), according to their analysis. Orland is a research associate at Goddard Space Flight Center and the University of Maryland, Baltimore County, and McCabe is a post-doctoral associate at the University of Maryland, College Park.

An estimated 19,000 people evacuated from areas threatened by the blazes, according to news reports. Many sought refuge in makeshift shelters such as schools, gymnasiums, and docked ships, while some in seaside villages boarded coast guard vessels to move to safety.

As of July 24, there were 82 fires burning across Greece, with 64 of those starting on July 23. In addition to the many people impacted on Rhodes, upwards of 2,500 people on Corfu were evacuated, and residents of villages in southern Evia found themselves in harm's way as high winds fanned the flames.

Fires are not unusual in Greece, but heat-stoked fire weather is projected to become more common as the planet warms. The intense fire season of 2021 came on the heels of extreme heat, and the number of fires and area burned in Greece were far above average. Experts think the current heat wave is set to become Greece's longest on record, with temperatures exceeding 40°C (104°F) for days on end in late July. The area burned by fires is more than double the average for this point in the year.

NASA's Earth Applied Sciences Disasters program area has been activated in support of the fires in Greece, responding to a request from the World Central Kitchen for data and imagery of the fires' location and impacts to inform their humanitarian efforts in setting up kitchens for those affected. As new information becomes available, the team will be posting maps and data products on its open-access mapping portal.

NASA Earth Observatory image by Lauren Dauphin, using Landsat data from the U.S. Geological Survey. Story by Lindsey Doermann. The image images can be viewed online by visiting the Landsat Image Gallery, https://landsat.gsfc.nasa.gov/, image id 151628.

asprs

THE IMAGING & GEOSPATIAL INFORMATION SOCIETY

PHOTOGRAMMETRIC ENGINEERING & REMOTE SENSING

Journal Staff

Publisher ASPRS
Editor-In-Chief Alper Yilmaz
Director of Publications Rae Kelley
Electronic Publications Manager/Graphic Artist Matthew Austin

Photogrammetric Engineering & Remote Sensing is the official journal of the American Society for Photogrammetry and Remote Sensing. It is devoted to the exchange of ideas and information about the applications of photogrammetry, remote sensing, and geographic information systems. The technical activities of the Society are conducted through the following Technical Divisions: Geographic Information Systems, Photogrammetric Applications, Lidar, Primary Data Acquisition, Professional Practice, Remote Sensing Applications, and Unmanned Autonomous Systems. Additional information on the functioning of the Technical Divisions and the Society can be found in the Yearbook issue of *PE&RS*.

All written correspondence should be directed to the American Society for Photogrammetry and Remote Sensing, PO Box 14713, Baton Rouge, LA 70898, including general inquiries, memberships, subscriptions, business and editorial matters, changes in address, manuscripts for publication, advertising, back issues, and publications. The telephone number of the Society Headquarters is 225-408-4747; the fax number is 225-408-4422; web address is www.asprs.org.

PE&RS. *PE&RS* (ISSN0099-1112) is published monthly by the American Society for Photogrammetry and Remote Sensing, 8550 United Plaza Blvd, Suite 1001, Baton Rouge, Louisiana 70809 . Periodicals postage paid at Bethesda, Maryland and at additional mailing offices.

SUBSCRIPTION. *PE&RS* is available as an e-Subscription (single-site and multi-site licenses) and an e-Subscription with print add-on (single-site license only). PE&RS subscriptions are on a calendar-year, beginning in January and ending in December.

The rate for a single-site e-Subscription for the USA/Non-USA is $1040 USD, for Canadian* is $1092 USD.

The rate for a multi-site e-Subscription for the USA/Non-USA is $1040 USD plus $250 USD for each additional license, for Canadian* is $1092 USD plus $263 for each additional license.

The rate for e-Subscription with print add-on for the USA is $1525 USD, for Canadian* is $1612 USD, and for Non-USA is $1565 USD.

*Note: Subscription prices for Canada includes 5% of the total amount for Canada's Goods and Services Tax (GST #135123065). **PLEASE NOTE: All Subscription Agencies receive a 20.00 USD discount.**

POSTMASTER. Send address changes to PE&RS, ASPRS, PO Box 14713, Baton Rouge, LA 70898. CDN CPM #(40020812).

MEMBERSHIP. Membership is open to any person actively engaged in the practice of photogrammetry, photointerpretation, remote sensing and geographic information systems; or who by means of education or profession is interested in the application or development of these arts and sciences. Membership is for one year, with renewal based on the anniversary date of the month joined. Membership Dues include a 12-month electronic subscription to *PE&RS*. Annual Individual Membership dues are $175.00 USD and Student Membership dues are $50.00 USD. A tax of 5% for Canada's Goods and Service Tax (GST #135123065) is applied to all members residing in Canada.

The ASPRS Positional Accuracy Standards, Edition 2: The Geospatial Mapping Industry Guide to Best Practices

By Qassim Abdullah, Ph.D., PLS, CP, Woolpert Vice President and Chief Scientist

The geospatial industry is fortunate to have the American Society for Photogrammetry and Remote Sensing to safeguard and advance industry best practices and proper conduct. The ASPRS Positional Accuracy Standards for Digital Geospatial Data of 2014 were the first accuracy standards developed for digital mapping practices and have provided the beacon for this guidance.

The ASPRS Positional Accuracy Standards for Digital Geospatial Data, Edition 2, was approved by the ASPRS Board of Directors on August 23, 2023. This edition was developed through observations and feedback over the last seven years. It became apparent that a new edition of the standards was needed to incorporate recommendations, correct outdated guidelines, and to address quickly evolving sensors, technologies, and industry practices.

This article will highlight the main features of the standards and note the changes introduced in Edition 2. It will also help readers understand the new standards and how they apply to everyday mapping activities.

Edition 2 was developed by community consensus, with specialists from private companies, public agencies, and academia contributing to its development. For the first time, four state departments of transportation contributed to these standards. This paradigm of participation was created to expand the standards to the wider community of mapping, remote sensing, and engineering practices.

Photogrammetric Engineering & Remote Sensing
Vol. 89, No. 10, October 2023, pp. 581-588.
0099-1112/22/581-588

doi: 10.14358/PERS.89.10.581

Motivation Behind the New ASPRS Accuracy Standards

- Legacy map accuracy standards, such as the U.S. National Map Accuracy Standards (NMAS) of 1947 and ASPRS 1990 standards, have become outdated.
- Many of the data acquisition and mapping technologies that these standards were based on are no longer used.
- Recent advances in mapping technologies can produce better quality and higher accuracy geospatial products and maps.
- Legacy map accuracy standards were designed with only plotted or drawn maps to represent geospatial data.
- Within the past two decades, as the industry transitioned between hardcopy and softcopy mapping environments, most standard measures for relating ground sample distance (GSD) and map scale to the final mapping accuracy were inherited from photogrammetric practices using scanned film.
- New mapping processes and methodologies have become much more sophisticated with advances in technology and in our knowledge of mapping processes and mathematical modeling.
- Mapping accuracy can no longer be associated with camera geometry and flying altitude alone (focal length, xp, yp, B/H ratio, etc.)
- Elevation products from the new technologies and active sensors—such as lidar, UAS, and IFSAR—are not covered in the legacy mapping standards. New accuracy standards are needed to address elevation products derived from these technologies.
- Today's mapping accuracy is influenced by many factors, such as:
  - The quality of camera calibration parameters.
  - Quality and size of a charged coupled device (CCD) used in the digital camera CCD array.
  - Amount of imagery overlap.
  - Quality of parallax determination or photo measurements.
  - Quality of the GPS signal.
  - Quality and density of ground controls.
  - Quality of the aerial triangulation solution.
  - Capability of the processing software to handle GPS drift and shift.
  - Capability of the processing software to handle camera self-calibration.
  - The digital terrain model used to produce orthoimagery.

These factors can vary widely from project to project, depending on the sensor used and specific methodology. For these reasons, existing accuracy measures based on map scale, film scale, GSD, c-factor, and scanning resolution no longer apply to current geospatial mapping practices.

New Standards for a New Era

While old standards guided the initial practices of mapmaking that were based on paper map media and film cameras, new digital sensor technologies like lidar, digital cameras, and geospatial products and practices challenged these standards.

Highlights of the New Standards Include:

- Sensor agnostic, data driven.
- Designed for today's digital sensors and mapping practices.
- Positional accuracy measure that is based on ground measurement units, not map units.
- Positional accuracy thresholds that are independent of published GSD, map scale or contour interval.
- It is all metric!
- Unlimited horizontal and vertical accuracy classes to support any sensor technology.
- Based on root mean square error (RMSE) alone as an accuracy indicator.
- Provide additional accuracy measures such as:
  - Aerial triangulation accuracy
  - Ground control accuracy
  - Orthoimagery seam lines accuracy
  - Lidar relative swath-to-swath accuracy
  - Independent checkpoint accuracy
- Provide recommended minimum nominal pulse density (NPD) for lidar data.
- Provide a measure for horizontal accuracy for elevation data.
- Provide guidelines on number and spatial distribution of checkpoints based on project area.
- Introduce the new 3D accuracy measure.
- Provide five addenda on guidelines and best practices for various mapping techniques.
- Ease of use and application. Once the user defines the product's accuracy, the standards set the rest of the requirements for the intermediate processes that are involved in producing the final products. An example of that is that users can specify the required product accuracy and the standards will set all requirements for aerial triangulation accuracy, ground control point accuracy, checkpoint accuracy, etc. The figure below illustrates this characteristic of the new standards.

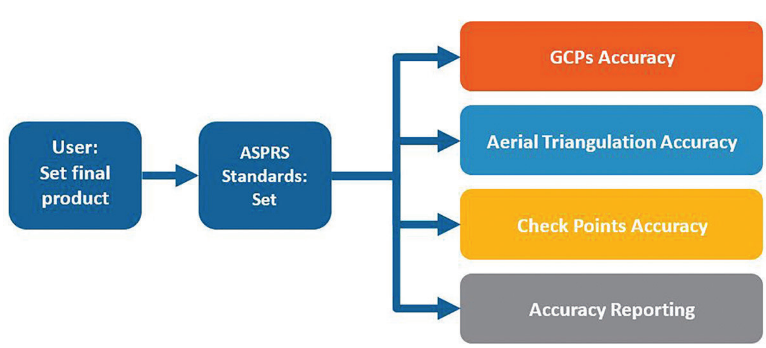

Introducing Edition 2

In 2022, ASPRS established a formal Positional Accuracy Standards Working Group under the Standards Committee to evaluate user comments and consider technology advancements to implement appropriate changes to the standards. Based on the feedback received from the industry and the advances the industry has witnessed in sensor technologies and best practices, the following important changes were introduced in Edition 2:

Change #1—Relaxed Accuracy Requirement for Ground Control and Checkpoints

As demand for geospatial products with higher accuracy increases, the accuracy requirements for the surveyed ground control and checkpoints have increased accordingly. According to Edition 1 of the standards, the accuracy of ground controls required for photogrammetric work needs to be four times better than the produced products, and checkpoints need to be three times better than the assessed product.

Advances in today's sensor technologies, processing software and algorithms, and processing methodology are enabling us to produce more accurate products. Therefore, we no longer need the three or four times "safety factor" to ensure the desired accuracy of the delivered products. In addition, imposing such restrictive requirements for the ground control and checkpoint surveys presented a burden on field surveying practices when using Global Navigation Satellite System (GNSS) techniques. Real-time kinematic (RTK)-based surveys also became ineligible to support some high-accuracy products, like the U.S. Geological Survey's Quality Level 0 lidar.

Change #2—Eliminated References to 95% Confidence Level as Accuracy Measure

The 95% confidence measure of accuracy for geospatial data was introduced in the National Standard for Spatial Data Accuracy (NSSDA), published by the Federal Geographic Data Committee in 1998. This measure was carried forward in the ASPRS Guidelines for Vertical Accuracy Reporting for Lidar Data published in 2004, as well as in Edition 1 of these standards.

Although Edition 1 endorses the use of RMSE as the main accuracy measure, it also references the 95% confidence level throughout. Experience has shown that reporting two quantities that represent the same accuracy at different confidence levels creates confusion for users and data producers alike. Users cannot compute accuracy at a 95% confidence level without computing RMSE first, therefore there is no need for a second accuracy that is derived from the first accuracy. The RMSE is a straightforward accuracy measure that is easy to understand and compute.

Change #3—Required Inclusion of Survey Checkpoint Accuracy when Computing Accuracy of Final Product

Since checkpoints and control points are no longer needed to meet the three or four times the intended product accuracy and demands for high-accuracy products are on the rise, errors in the surveyed checkpoints used to assess final product accuracy, although small, can no longer be neglected. As product accuracy increases, the impact of error in checkpoints on the computed product accuracy increases. When final products are used for further measurements, calculations, or decision-making, the reliability of these subsequent measurements can be better estimated if the uncertainty associated with the checkpoints or control points is factored in.

Change #4—Removed Pass/fail Requirement for Vegetated Vertical Accuracy for Lidar Data

Data producers and data users reported that they were challenged in situations where Non-Vegetated Vertical Accuracy (NVA) is well within contract specifications, but Vegetated Vertical Accuracy (VVA) is not. Since VVA is influenced by factors that fall outside the lidar system accuracy, it is fair to all parties involved in a contract to base the data acceptance or rejection decision for the overall project on the quality of the tested NVA.

In most cases, the VVA assessment is compromised and the quality of lidar-derived surface under trees is affected due to the following reasons:

1. Vegetation blocks the lidar pulse from reaching the ground, resulting in less-than-perfect density of the point cloud representing the terrain.
2. The compromised density of lidar points reaching the ground under trees results in poor modeling of the terrain where the checkpoints are located,
3. The performance of algorithms used to separate underground and above-ground points in vegetated areas.
4. The quality of GPS-based surveying techniques in vegetated areas is compromised due to restricted satellite visibility and multipath issues.

Edition 2 calls for the VVA to be evaluated and reported as it is found, but it should not be used as a criterion for rejection or acceptance.

Change #5—Increased Minimum Number of Checkpoints Required for Product Accuracy Assessment from 20 to 30

In Edition 1, a minimum of 20 checkpoints was required for testing positional accuracy of a final mapping product. This minimum was not based on rigorous science or statistical theory, but was a holdover from NMAS of 1947, published by the U.S. Bureau of the Budget.

In Edition 2, a better scientific approach is introduced based on a well-respected theorem in statistics, the central limit theorem. According to the central limit theorem, regardless of the distribution of the population, if the sample size is sufficiently large (n ≥ 30), then the sample mean is approximately normally distributed, and the normal probability model can be used to quantify uncertainty when making inferences about a population based on the sample mean. Therefore, in Edition 2 a product accuracy assessment must have a minimum number of 30 checkpoints to be considered fully compliant.

Change #6—Limited Maximum Number of Checkpoints for Large Projects to 120

According to Edition 1 guidelines, large projects require hundreds, sometimes thousands of checkpoints to assess product accuracy. These numbers have proved to be unrealistic for the industry, as they inflate project budgets and, in some cases, hinder project executions—especially for projects in remote or difficult-to-access areas.

Since Edition 2 recognizes the central limit theorem as the basis for statistical testing, there is insufficient evidence to support the need to increase the number of checkpoints indefinitely as the project area increases. The new maximum number of 120 checkpoints is equal to four times the number cited by the central limit theorem, and that should provide a statistically valid sample.

Change #7—Introduced New Accuracy Term: "Three-dimensional Positional Accuracy."

Three-dimensional models and digital twins are gaining acceptance in many engineering and planning applications. Many future geospatial data sets will be in true 3D form. Therefore, a method for assessing positional accuracy of a point or feature within a 3D model is needed to support future innovation and product specifications. 3D models require 3D accuracy, rather than separate horizontal and vertical accuracies. Edition 2 endorses the use of the following three terms:

- Horizontal positional accuracy
- Vertical positional accuracy
- 3D positional accuracy

Change #8—Added Addenda on Best Practices and Guidelines

With geospatial mapping practices and technologies evolving quickly, users need guidelines on how to keep up. In response, Edition 2 introduces the following five addenda:

Addendum I: General Best Practices and Guidelines
Addendum II: Best Practices and Guidelines for Field Surveying of Ground Control and Checkpoints
Addendum III: Best Practices and Guidelines for Mapping with Photogrammetry
Addendum IV: Best Practices and Guidelines for Mapping with Lidar
Addendum V: Best Practices and Guidelines for Mapping with UAS

Understanding Edition 2 of the ASPRS Positional Accuracy Standards for Digital Geospatial Data

Horizontal Positional Accuracy Standard for Geospatial Data

The standards specify horizontal accuracy classes as they relate to digital orthoimagery, digital planimetric data, scaled planimetric maps, and elevation data in terms of $RMSE_H$, which is the combined linear error along a horizontal plane in the radial direction. $RMSE_H$ is derived from $RMSE_X$ and $RMSE_Y$ according to the following formula:

$$RMSE_H = \sqrt{{RMSE_X}^2 + {RMSE_Y}^2}$$

In the case of digital orthoimagery mosaics, an additional criterion for the allowable mismatch at seamlines of ≤ 2* $RMSE_H$ is specified in Table 1. The term $RMSE_H$ should be computed using both $RMSE_{H_1}$ and $RMSE_{H_2}$ error components, as will be illustrated in the next sections.

Table 1. Horizontal Positional Accuracy Standard for Geospatial Data.

Horizontal Accuracy Class	Absolute Accuracy	Orthoimagery Mosaic Seamline Mismatch (cm)
	$RMSE_H$ (cm)	
#-cm	≤ #	≤ 2*#

Vertical Positional Accuracy Standard for Elevation Data

Vertical accuracy is to be expressed as $RMSE_V$ in both vegetated and non-vegetated terrain. Vertical accuracy classes are defined by the associated $RMSE_V$ specified for the product. The term $RMSE_V$ should be computed using both $RMSE_{V_1}$ and $RMSE_{V_2}$ error components, as will be illustrated in the next sections. While the NVA must meet accuracy thresholds listed in Table 2, the VVA does not and needs only to be tested and reported as found. If the NVA meets user specifications, the VVA should be accepted at the reported accuracy level. Table 2 shows the vertical accuracy class specifications for digital elevation data, including Data Internal Precision requirements where applicable, such as in lidar.

Table 2. Vertical Positional Accuracy Standard for Geospatial Data.

Vertical Accuracy Class	Absolute Accuracy		Data Internal Precision (where applicable)		
	NVA $RMSE_V$ (cm)	VVA $RMSE_V$ (cm)	Within-Swath Smooth Surface Precision Max Diff (cm)	Swath-to-Swath Non-Vegetated RMS_{DZ} (cm)	Swath-to-Swath Non-Vegetated Max Diff (cm)
#-cm	≤ #	*As found*	*≤ 0.60*#*	*≤ 0.80*#*	*≤ 1.60*#*

3D Positional Accuracy Standard for Geospatial Data

3D positional accuracy can be computed for any type of geospatial data, as long as the horizontal and vertical positional accuracy are assessed and reported. It is especially useful in assessing accuracy for colorized point clouds and digital twins. Table 3 defines the 3D accuracy standard for any 3D digital data as a combination of horizontal and vertical radial error. $RMSE_{3D}$ is derived from the horizontal and vertical components of error according to the following formula:

$$RMSE_{3D} = \sqrt{{RMSE_X}^2 + {RMSE_Y}^2 + {RMSE_Z}^2}$$

or,

$$RMSE_{3D} = \sqrt{{RMSE_H}^2 + {RMSE_V}^2}$$

Table 3. 3D Positional Accuracy Standard for Geospatial Data.

3D Accuracy Class	Absolute Accuracy
	$RMSE_{3D}$ (cm)
#-cm	≤ #

Horizontal Accuracy of Elevation Data

The standards outline horizontal accuracy testing requirements for elevation data created from stereo photogrammetry and lidar. For other technologies, appropriate horizontal accuracies for elevation data should be negotiated between the data producer and the client, with specific accuracy thresholds and methods based on the technology used and the project design. Horizontal accuracy for elevation data is determined using one of the following approaches:

- **Photogrammetric elevation data:** For elevation data derived using stereo photogrammetry, apply the same horizontal accuracy class that would be used for planimetric data or digital orthoimagery produced from the same source, based on the same photogrammetric adjustment.
- **Lidar elevation data**: The standards provide the following equation to estimate the horizontal accuracy for a lidar-derived dataset ($RMSE_H$), based on the main errors introduced by the positional accuracy of the GNSS; roll, pitch, and heading accuracy of the inertial measurement unit (IMU); and the flying height:

$$RMSE_H = \sqrt{(GNSS\ positional\ error)^2 + \left(\frac{\tan(IMU\ roll\ or\ pitch\ error) + \tan(IMU\ heading\ error)}{1.478} * flying\ height\right)^2}$$

Using the above equation, the horizontal accuracy of lidar data acquired from different flying altitude are listed in Table 4.

Table 4. Estimated Horizontal Error (RMSEH) in Lidar Data as a Function of GNSS Error, IMU Error, and Flying Height.

Flying Height (m)	GNSS Error (cm)	IMU Roll/Pitch Error (arc-sec)	IMU Heading Error (arc-sec)	$RMSE_H$ (cm)
500	*10*	*10*	*15*	*10.7*
1,000	*10*	*10*	*15*	*12.9*
1,500	*10*	*10*	*15*	*15.8*
2,000	*10*	*10*	*15*	*19.2*
2,500	*10*	*10*	*15*	*22.8*
3,000	*10*	*10*	*15*	*26.5*
3,500	*10*	*10*	*15*	*30.4*
4,000	*10*	*10*	*15*	*34.3*
4,500	*10*	*10*	*15*	*38.2*
5,000	*10*	*10*	*15*	*42.0*

Accuracy Requirements for Aerial Triangulation and IMU-Based Sensor Orientation

The quality and accuracy of the aerial triangulation, if performed, and/or the GNSS/IMU-based direct georeferencing play key roles in determining the final accuracy of imagery-derived mapping products.

- For aerial triangulation designed for digital planimetric data (orthoimagery and/or map) only:

  $RMSE_{H1(AT)} \le ½ * RMSE_{H(MAP)}$

  $RMSE_{V1(AT)} \le RMSE_{H(MAP)}$

- For aerial triangulation designed for projects that include elevation or 3D products, in addition to digital planimetric data (orthoimagery and/or map):

  $RMSE_{H1(AT)} \le ½ * RMSE_{H(MAP)}$

  $RMSE_{V1(AT)} \le ½ * RMSE_{V(DEM)}$

The ASPRS Positional Accuracy Standards for Digital Geospatial Data of 2014 were the first accuracy standards developed for digital mapping practices and have provided the beacon for this guidance

Accuracy Requirements for Ground Control Used for Aerial Triangulation

The accuracy of the ground control points should be twice the target accuracy of the final products, according to the following two categories:

- Ground control for aerial triangulation designed for digital planimetric data (orthoimagery and/or map) only:

  $RMSE_{H(GCP)} \leq ½ * RMSE_{H(MAP)}$

  $RMSE_{V(GCP)} \leq RMSE_{H(MAP)}$

- Ground control for aerial triangulation designed for projects that include elevation or 3D products, in addition to digital planimetric data (orthoimagery and/or map):

  $RMSE_{H(GCP)} \leq ½ * RMSE_{V(MAP)}$

  $RMSE_{V(GCP)} \leq ½ * RMSE_{H(DEM)}$

Accuracy Requirements for Ground Control Used for Lidar

The accuracy of the ground control points used for lidar calibration and boresighting should be twice the target accuracy of the final products. Similarly, ground checkpoints used to assess lidar data accuracy should be twice the target accuracy of the final products.

$RMSE_{V(GCP)} \leq ½ * RMSE_{V(DEM)}$

Similar guidelines can be followed for other digital data acquisition technologies, such as IFSAR.

Reporting Geospatial Data Accuracy

Knowing the positional accuracy of a geospatial product is important, as it plays a great role in determining the applicability of the data for an intended purpose. Mislabeled or poorly reported positional accuracy can have catastrophic consequences. Therefore, the geospatial data exchanged among users should be accompanied by metadata clearly stating its positional accuracy. To help data users and data producers, Edition 2 provides formal accuracy reporting statements that serve different scenarios.

Number and Distribution of Checkpoints for Horizontal Accuracy and NVA Assessment

According to Edition 2, a minimum of 30 checkpoints are needed to assess the horizontal and non-vegetated vertical accuracy of a dataset. A large project, or more than 1,000 square kilometers, will need more checkpoints. Table 5 lists the recommended number of checkpoints according to the project size.

Table 5 recommends the use of a minimum of 30 checkpoints for a project area of 1,000 square kilometers or less and a maximum of 120 checkpoints for a project area larger than 10,000 square kilometers. Checkpoints should be evenly distributed across the project area as much as possible.

[1] For very small projects where the use of 30 checkpoints is not feasible, report the accuracy as suggested in section 7.15.

Table 5. Recommended Number of Checkpoints for Horizontal Accuracy and NVA Testing Based on Project Area.

Project Area (Square Kilometers)	Total Number of Checkpoints for NVA
≤1000[1]	30
1001-2000	40
2001-3000	50
3001-4000	60
4001-5000	70
5001-6000	80
6001-7000	90
7001-8000	100
8001-9000	110
9001-10000	120
>10000	120

Considerations made for challenging circumstances—such as rugged terrain, water bodies, heavy vegetation, and inaccessibility—are acceptable if agreed upon between the data producer and the client. Details on the best locations for these checkpoints are provided in section 7.12 of the standards.

Testing VVA

If the project requires the VVA to be tested, there should be a minimum of 30 VVA checkpoints regardless of the project area. The data user and data producer may agree to collect a larger number of checkpoints. To avoid situations where errors in checkpoints in the vegetated terrain do not follow a random distribution, no combined statistical terms, such as $RMSE_V$, should be used in evaluating the results of the test. In other words, only individual elevation differences (i.e., errors) for each checkpoint shall be used in the evaluation.

Accuracy of Checkpoints

According to Edition 2, checkpoints used to assess any product accuracy (horizontal, vertical, or 3D) should be twice as accurate as the test products.

Testing and Reporting of Product Accuracy:

New to the standards is the way accuracy is computed. The following formula represents the updated and accepted method for computing product accuracy:

$$Horizontal\ Product\ Accuracy\ (RMSE_H) = \sqrt{{RMSE_{H_1}}^2 + {RMSE_{H_2}}^2}$$

$$Vertical\ Product\ Accuracy\ (RMSE_V) = \sqrt{{RMSE_{V_1}}^2 + {RMSE_{V_2}}^2}$$

$$RMSE_{3D} = \sqrt{{RMSE_H}^2 + {RMSE_V}^2}$$

Where:

$RMSE_H$, $RMSE_V$, and $RMSE_{3D}$ are the product's horizontal, vertical, and 3D accuracy, respectively.

$RMSE_{H_1}$ and $RMSE_{V_1}$ are the components of error derived from product fit to the checkpoints.

$RMSE_{H_2}$ and $RMSE_{V_2}$ are are the components of error associated with checkpoint surveys.

For the purposes of demonstration, suppose you were provided with five checkpoints to verify the final horizontal and vertical accuracy for a dataset (this example uses fewer checkpoints than the minimum 30 for the sake of brevity) according to these standards.

Table 6 provides the map-derived coordinates and the surveyed coordinates for the five points. The table also shows the computed accuracy and other relevant statistics. In this abbreviated example, the data are intended to meet a target horizontal accuracy class of $RMSE_H$ = 15cm and a target vertical accuracy class of $RMSE_V$ = 10cm.

Computation of Horizontal, Vertical, and 3D Accuracy

1. Compute the RMSE values:

$$RMSE_x = \sqrt{\frac{1}{n}\sum_{i=1}^{n}(x_{i(map)} - x_{i(surveyed)})^2}$$

where:

$x_{i(map)}$ is the coordinate in the specified direction of the i^{th} checkpoint in the dataset,

$x_{i(surveyed)}$ is the coordinate in the specified direction of the i^{th} checkpoint in the independent source of higher accuracy,

n is the number of checkpoints tested,

and i is an integer ranging from 1 to n.

$$RMSE_x = \sqrt{\frac{(-0.140)^2+(-0.100)^2+(0.017)^2+(-0.070)^2+(0.130)^2}{5}} = 0.102 \text{ m}$$

$$RMSE_y = \sqrt{\frac{(-0.070)^2+(-0.100)^2+(-0.070)^2+(0.150)^2+(0.120)^2}{5}} = 0.107 \text{ m}$$

$$RMSE_{H_1} = \sqrt{RMSE_x{}^2 + RMSE_y{}^2}$$

$$RMSE_{H_1} = \sqrt{(0.102)^2 + (0.107)^2} = 0.147 \text{ m}$$

$$RMSE_{V_1} = \sqrt{\frac{(-0.071)^2+(0.010)^2+(0.102)^2+(-0.100)^2+(0.087)^2}{5}} = 0.081 \text{ m}$$

Edition 2 was developed through observations and feedback over the last seven years. It became apparent that a new edition of the standards was needed to incorporate recommendations, correct outdated guidelines, and to address quickly evolving sensors, technologies, and industry practices.

2. Compute the final accuracy values:

To complete the accuracy computations, let us assume that the checkpoint report submitted by the surveyor states that the field survey was conducted using an RTK-GPS-based technique to an accuracy of:

Horizontal accuracy $RMSE_{H_2}$ = 1.9cm or 0.019m

Vertical accuracy $RMSE_{V_2}$ = 2.23cm or 0.022m

Table 6. Accuracy Statistics for Example Data.

Point ID	Map-derived Values			Surveyed Checkpoints Values			Residuals (Errors)		
	Easting (E)	Northing (N)	Elevation (Z)	Easting (E)	Northing (N)	Elevation (Z)	ΔE (Easting)	ΔN (Northing)	ΔZ (Elevation)
	meter	meter	meter	meter	meter	meter	meter	meter	meter
GCP1	359584.394	5142449.934	477.127	359584.534	5142450.004	477.198	-0.140	-0.070	-0.071
GCP2	359872.190	5147939.180	412.406	359872.290	5147939.280	412.396	-0.100	-0.100	0.010
GCP3	359893.089	5136979.824	487.292	359893.072	5136979.894	487.190	0.017	-0.070	0.102
GCP4	359927.194	5151084.129	393.591	359927.264	5151083.979	393.691	-0.070	0.150	-0.100
GCP5	372737.074	5151675.999	451.305	372736.944	5151675.879	451.218	0.130	0.120	0.087
						Number of check points	5	5	5
						Mean Error (m)	-0.033	0.006	0.006
						Standard Deviation (m)	0.108	0.119	0.091
						RMSE (m)	0.102	0.106	0.081
						Fit to Checkpoints $RMSE_{H1}$ (m)	0.147	$RMSE_H = \sqrt{RMSE_E{}^2 + RMSE_N{}^2}$	
						Fit to Checkpoints $RMSE_{V1}$ (m)	0.081		

The final horizontal and vertical accuracy should be computed as follows:

$$RMSE_H = \sqrt{{RMSE_{H_1}}^2 + {RMSE_{H_2}}^2} = \sqrt{(0.147)^2 + (0.019)^2} = 0.148 \text{ m } (< 15 \text{ cm})$$

$$RMSE_V = \sqrt{{RMSE_{V_1}}^2 + {RMSE_{V_2}}^2} = \sqrt{(0.081)^2 + (0.022)^2} = 0.083 \text{ m } (< 10 \text{ cm})$$

Similarly, the 3D positional accuracy can be computed using the following formula:

$$RMSE_{3D} = \sqrt{{RMSE_H}^2 + {RMSE_V}^2}$$

Therefore,

$$RMSE_{3D} = \sqrt{0.148^2 + 0.083^2} = 0.170 \text{ m}$$

Based on the computed horizontal and vertical accuracy numbers above, the product is meeting the specified horizontal and vertical accuracies of 15cm and 10cm, respectively.

Final Notes

The material in this article is intended to shed light on important aspects of the new edition of the ASPRS Positional Accuracy Standards for Digital Geospatial Data. Readers are encouraged to review the standards for full clarity and edification. Edition 2, version 1.0 includes only two of the five addenda. The remaining three Addenda listed in the Table of Contents:

Addendum III: Best Practices and Guidelines for Mapping with Photogrammetry
Addendum IV: Best Practices and Guidelines for Mapping with Lidar
Addendum V: Best Practices and Guidelines for Mapping with UAS

will be available for public comment in the coming weeks and will be added to Edition 2, Version 2.0, which ASPRS anticipates approving in late Fall 2023.

To download Edition 2 document, visit https://publicdocuments.asprs.org/PositionalAccuracyStd-Ed2-V1

Acknowledgment

Dr. Qassim Abdullah would like to extend his gratitude to all individuals who assisted in drafting Edition 2 of the standards, especially members of the ASPRS Positional Accuracy Standards Working Group, Dr. Riadh Munjy of California State University, Fresno; Josh Nimetz of the USGS, Michael Zoltek of GPI Geospatial, Inc.; and Colin Lee of the Minnesota Department of Transportation. Additionally, he would like to recognize the teams who worked on drafting the addenda on best practices and guidelines, led by Jim Gillis of VeriDaaS Corporation; Dr. Sagar Deshpande of Dewberry; Dr. Nora May of Fugro; Jacob Lopez of Towill, Inc.; Dr. Christopher E. Parrish of Oregon State University; Martin Flood of GeoCue Group, Leo Liu of Inertial Labs, Munjy; and Zoltek. He would also like to extend his appreciation to the ASPRS staff under the leadership of Karen Schuckman, who was instrumental in reviewing the draft and providing valuable suggestions and comments. Abdullah said he is grateful to Alan Mikuni of GeoWing Mapping, Inc., who volunteered his time to proofread all drafts. Thank you, Alan, for doing a great job.

This article will be published concurrently in Lidar Magazine.

NEW ASPRS MEMBERS

ASPRS would like to welcome the following new members!

Gabriel Ahoma
David Andes
Gene Bailey
David Buback
DeAnna Clum
Dick Durstein
Mark S. Erickson
Safak Fidan
Hayden Fischer
Felipe Galindo, Sr.
Jason M. Gustafson
Jeffrey Hall
Jacob Heckert
Jared Jacobs
Steve Aury LeBlanc, PLS
Savannah Madden
David Miceli
William Middleton
Angelica M. Otting
Lindsey Rotche
Devlin Rutherford
Zach Saavedra
Claudette Sandoval-Green
Jill Schwarz, PhD
Carlina Wharton-Bucher
Lucas Wilsing

FOR MORE INFORMATION ON ASPRS MEMBERSHIP, VISIT
HTTP://WWW.ASPRS.ORG/JOIN-NOW

ASPRS Positional Accuracy Standards for Digital Geospatial Data

(EDITION 2, VERSION 1.0 - AUGUST 2023)

Foreword

Edition 1 of the ASPRS Positional Accuracy Standards for Digital Geospatial Data was published in November 2014. In the years since, users expressed concerns and suggested revisions based on their experience applying the Standards in real-world situations. In addition, technologies have evolved in such a way as to challenge the assumptions upon which Edition 1 was based.

In 2022, ASPRS established a formal Positional Accuracy Standards Working Group under the Standards Committee to evaluate user comments, consider technology advancements, and implement appropriate changes to the Standards. The following individuals were appointed to the Positional Accuracy Standards Working Group:

Chair: Dr. Qassim Abdullah, Vice President and Chief Scientist, Woolpert, Inc.

Members:

- Dr. Riadh Munjy, Professor of Geomatics Engineering, California State University, Fresno
- Josh Nimetz, Senior Elevation Project Lead, U.S. Geological Survey
- Michael Zoltek, National Geospatial Programs Director, GPI Geospatial, Inc.
- Colin Lee, Photogrammetrist, Minnesota Department of Transportation

The ASPRS Positional Accuracy Standards for Digital Geospatial Data are designed to be modular in nature, such that revisions could be made and additional sections added as geospatial technologies and methods evolve. Additionally, the Standards are designed to recommend best practices, methods, and guidelines for the use of emerging technologies to achieve the goals and requirements set forth in the Standards. With support from the ASPRS Technical Divisions, the primary Working Group established subordinate Working Groups to author Addenda for best practices and guidelines for photogrammetry, lidar, UAS, and field surveying. The subordinate Working Group members and contributors are credited in each Addendum, as appropriate.

Summary of Changes in Edition 2

Important changes adopted in Edition 2 of the Standards are as follows:

1. **Eliminated references to the 95% confidence level as an accuracy measure.**
   - **Reason for the change:** The 95% confidence measure of accuracy for geospatial data was introduced in the National Standard for Spatial Data Accuracy (NSSDA) published by the Federal Geographic Data Committee in 1998. This measure was carried forward in the ASPRS Guidelines for Vertical Accuracy Reporting for Lidar Data published in 2004, as well as in Edition 1 of the ASPRS Positional Accuracy Standards for Digital Geospatial Data published in 2014. However, RMSE is also a way to express data accuracy, and it is typically reported alongside the 95% confidence level because the two are derived from the same error distribution. As a matter of fact, users need to compute RMSE first in order to obtain the 95% confidence measure. The reporting of two quantities representing the same accuracy at different confidence levels has created confusion for users and data producers alike.
   - **Justification for the change:** The RMSE is a reliable statistical term that is sufficient to express product accuracy, and it is well understood by users. Experience has shown that the use of both RMSE and the 95% confidence level leads to confusion and misinterpretation.
2. **Relaxed the accuracy requirement for ground control and checkpoints.**
   - **Reason for the change:** Edition 1 called for ground control points of four times the accuracy of the intended final product, and ground checkpoints of three times the accuracy of the intended final product. With goals for final product accuracies approaching a few centimeters in both the horizontal and vertical, it becomes difficult, if not impossible, to use RTK methods for control and checkpoint surveys, introducing a significant burden of cost for many high-accuracy projects.

Photogrammetric Engineering & Remote Sensing
Vol. 89, No. 10, October 2023, pp. 589-592.
0099-1112/22/589-592

doi: 10.14358/PERS.89.10.589

- **Justification for the change:** As the demand for higher-accuracy geospatial products grows, accuracy requirements for the surveyed ground control and checkpoints set forth in Edition 1 exceed those that can be achieved in a cost-effective manner, even with high-accuracy GPS. Furthermore, today's sensors, software, and processing methods have become very precise, diminishing the errors introduced in data acquisition and processing. If best practices are followed, safety factors of three and four times the intended product accuracy are no longer needed.

3. **Required the inclusion of survey checkpoint accuracy when computing the accuracy of the final product.**
   - **Reason for the change:** Since checkpoints will no longer need to meet the three-times-intended-product accuracy requirement (see item 2 above), the error in the checkpoints survey may no longer be ignored when reporting the final product accuracy. This is especially important, given the increasing demand for highly accurate products—which, in some cases, approach the same order of magnitude as the survey accuracy of the checkpoints. Therefore, checkpoint error should be factored into the final product accuracy assessment that is used to communicate the reliability of resulting final products.
   - **Justification for the change:** Errors in the survey checkpoints used to assess final product accuracy, although small, can no longer be neglected. As product accuracy increases, the impact of error in checkpoints on the computed product accuracy increases. When final products are used for further measurements, calculations, or decision making, the reliability of these subsequent measurements can be better estimated if the uncertainty associated with the checkpoints is factored in.

4. **Removed the pass/fail requirement for Vegetated Vertical Accuracy (VVA) for lidar data.**
   - **Reason for the change:** Data producers and data users have reported that they are challenged in situations where Non-Vegetated Vertical Accuracy (NVA) is well within contract specifications, but VVA is not. As explained below, factors affecting VVA are not a function of the lidar system accuracy; therefore, only NVA should be used when making a pass/fail decision for the overall project. VVA should be evaluated and reported, but should not be used as a criterion for acceptance.
   - **Justification for the change:** Where lidar can penetrate to bare ground under trees, the accuracy of the points, as a function of system accuracy, should be comparable to lidar points in open areas. However, the accuracy and the quality of lidar-derived surface under trees is affected by:
     1. the type of vegetation where it affects the ability of lidar pulse to reach the ground,
     2. the density of lidar points reaching the ground,
     3. and the performance of the algorithms used to separate ground and above-ground points in these areas.

     Furthermore, the accuracy of the ground checkpoints acquired with GPS surveying techniques in vegetated areas is affected by restricted satellite visibility. As a result, accuracies computed from the lidar-derived surface in vegetated areas are not valid measures of lidar system accuracy.

5. **Increased the minimum number of checkpoints required for product accuracy assessment from 20 to 30.**
   - **Reason for the change:** In Edition 1, a minimum of 20 checkpoints are required for testing positional accuracy of the final mapping products. This minimum number is not based on rigorous science or statistical theory; rather, it is a holdover from legacy Standards and can be traced back to the National Map Accuracy Standards published by the U.S. Bureau of the Budget in 1947.
   - **Justification for the change:** The Central Limit Theorem calls for at least 30 samples to calculate statistics such as mean, standard deviation, and skew. These statistics are relied upon in positional accuracy assessments. According to The Central Limit Theorem, regardless of the distribution of the population, if the sample size is sufficiently large ($n \geq 30$), then the sample mean is approximately normally distributed, and the normal probability model can be used to quantify uncertainty when making inferences about a population based on the sample mean. Therefore, in Edition 2, a product accuracy assessment must have a minimum number of 30 checkpoints in order to be considered fully compliant.

6. **Limited the maximum number of checkpoints for large projects to 120.**
   - **Reason for the change:** Since these Standards recognize the Central Limit Theorem as the basis for statistical testing, there is insufficient evidence for the need to increase the number of checkpoints indefinitely as the project area increases. The new maximum number of checkpoints is equal to four times the number called by the Central Limit Theorem.
   - **Justification for the change:** According to the old guidelines, large projects require hundreds, sometimes thousands of checkpoints to assess product accuracy. Such numbers have proven to be unrealistic for the industry, as it inflates project budget and, in some cases, hinders project executions, especially for projects taking place in remote or difficult-to-access areas.

7. **Introduced a new accuracy term: "three-dimensional positional accuracy."**
   - **Reason for the change:** Three-dimensional models require consideration of three-dimensional accuracy,

rather than separate horizontal and vertical accuracies. Edition 2 endorses the use of the following three terms:
  - Horizontal positional accuracy
  - Vertical positional accuracy
  - Three-dimensional (3D) positional accuracy
- **Justification for the change:** Three-dimensional models and digital twins are gaining acceptance in many engineering and planning applications. Many future geospatial data sets will be in true three-dimensional form; therefore, a method for assessing positional accuracy of a point or feature within the 3D model is needed to support future innovation and product specifications.

8. Added Best Practices and Guidelines Addenda for:
  - General Best Practices and Guidelines
  - Field Surveying of Ground Control and Checkpoints
  - Mapping with Photogrammetry
  - Mapping with Lidar
  - Mapping with UAS

This summarizes the most significant changes implemented in Edition 2 of the ASPRS Positional Accuracy Standards for Digital Geospatial Data. Other minor changes will be noted throughout.

TABLE OF CONTENTS

FIGURES

TABLES

Dewberry is a leading, market-facing firm with a proven history of providing professional services to public- and private-sector clients. Established in 1956 and headquartered in Fairfax, Virginia, our professionals are dedicated to solving clients' most complex challenges and transforming their communities. The firm harnesses the power of geospatial science to offer complete end-to-end remote sensing and mapping services starting with state-of-the-art airborne lidar sensors to automated processing, surveying, web/mobile GIS, and advanced data analytics. Dewberry creates, analyzes, and builds geospatial data and tools, to help clients integrate, share, and simplify the use of information allowing for more effective and efficient decision making.

Dewberry's geospatial and technology services team includes more than 250 professionals who create, analyze, and build tools to share geospatial data, and help clients integrate these tools into their daily lives. By fusing multiple data sets together for more efficient data mining, Dewberry provides clients with easy-to-use tools that simplify the use of information to allow for more effective and efficient decision making.

Dewberry recently acquired a new topobathymetric lidar sensor–the RIEGL VQ-880-G II–to add to its growing inventory of lidar sensors. This marks the second topobathymetric sensor acquired by Dewberry, the first being a Teledyne CZMIL SuperNova, a unique sensor specially made for obtaining deep returns up to ~3.5 Secchi depth. Operating these two sensors provides the firm immense flexibility to map in a wide variety of aquatic environments and conditions. Dewberry has the ability to tailor its topobathymetric lidar acquisition to fit the strengths of these two systems. Additionally, the firm's RIEGL VQ 1560 IIS topographic lidar sensor adds to its breadth of mapping capabilities by offering high-density lidar collection over land. The firm is excited to empower their clients with access to the most innovative technology to meet their topographic/lidar needs, delivering hi-definition lidar datasets quickly and efficiently.

Dewberry has also implemented two initiatives to facilitate client communication and data processing efficiency. The firm is using Esri-powered, client-facing dashboards combined with quick-look technology, allowing clients to view data acquisition in near real-time and be an active partner in remote sensing activities. The second initiative focuses on improved feature extraction efficiency through automation. Dewberry's IT-team built custom multi-threaded, extended-memory computers dedicated for artificial intelligence (AI)/machine learning (ML) processing. These computers are used for feature extraction and automated classification of lidar data. This AI/ML workflow increases efficiency and decreases delivery time of geospatial products to clients.

Dewberry has received industry-wide recognition winning back-to-back year awards from Esri, the Management Association for Private Photogrammetric Surveyors (MAPPS), and the American Council of Engineering Companies (ACEC) in 2021, 2022, and 2023.

DimensionalView® is a multi-use tool developed in-house that can be used for real-time tracking not only for topobathymetric lidar acquisition, but for acquisition of various data types acquired with a wide variety of sensors and platforms. The platform can be used for topographic lidar, sonar, and aerial imagery to name a few. Another helpful layer that can be included in the portal are ground survey checkpoints, both for planning points and displaying final collected points. The tracker is a powerful project management tool that combines numerous data points into one web-based location and then adds easy-to-use geospatial features allowing the user to access the information they need in the format they need.

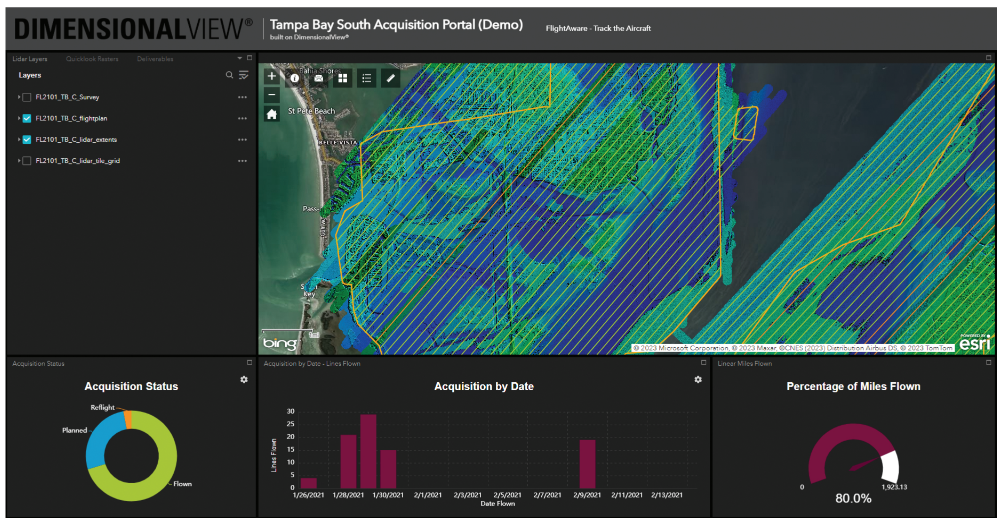

DimensionalView® is a multi-use tool developed in-house that can be used for real-time tracking not only for topobathymetric lidar acquisition, but for acquisition of various data types acquired with a wide variety of sensors and platforms.

Dewberry works seamlessly to provide geospatial mapping and technology services (GTS) across various market segments. With nearly 50 years of GTS experience, the firm is dedicated to understanding and applying the latest tools, trends, and technologies. Dewberry employs the latest GIS software and database platforms, including the full suite of ESRI products. The firm's products and services include application, web, and cloud-based development; system integration; database design mapping; data fusion; and mobile solutions. To learn more, visit www.dewberry.com.

Dewberry
Amar Nayegandhi
1000 North Ashley Drive, Suite 801, Tampa, FL 33602-3718
813.421.8642 | anayegandhi@dewberry.com
www.dewberry.com

Dewberry®

STAND OUT FROM THE REST

EARN ASPRS CERTIFICATION

ASPRS congratulates these recently Certified and Re-certified individuals:

RECERTIFIED PHOTOGRAMMETRIST

Michael Scanlan, Certification #R1531CP
Effective July 25, 2022, expires July 25, 2027

Joseph Bartorelli, Certification #R1367CP
Effective August 7, 2023, expires August 7, 2028

Christopher Aldridge, Certification #R1163CP
Effective August 28, 2023, expires August 28, 2028

Theodore Schall, Certification #R1357CP
Effective April 7, 2023, expires April 7, 2028

Craig Sweitzer, Certification #R1633CP
Effective June 13, 2023, expires June 13, 2028

Christopher Howell, Certification #R1641CP
Effective July 10, 2023, expires July 10, 2028

Sara Reed, Certification #R1634CP
Effective July 25, 2023, expires July 25, 2028

Alan Mikuni, Certification #R1127CP
Effective October 19, 2023, expires October 19. 2028

Jaime Higgins, Certification #R1635CP
Effective August 4, 2023, expires August 4, 2028

RECERTIFIED PHOTOGRAMMETRIST TECHNOLOGIST

Matthew Peloquin, Certification #R1649PT
Effective June 19, 2023, expires June 19, 2026

RECERTIFIED CERTIFIED MAPPING SCIENTIST GIS/LIS

Luis Ramos, Certification #R202GS
Effective June 2, 2023, expires June 2, 2028

RECERTIFIED CERTIFIED MAPPING SCIENTIST LIDAR

Larry Holtgreive, Certification #R037L
Effective February 4, 2024, expires February 4, 2029

RECERTIFIED LIDAR TECHNOLOGIST

Christian Sovak, Certification #R054LT
Effective July 17, 2023, expires July 17, 2026

CERTIFIED LIDAR TECHNOLOGIST

Travis Gannon, Certification #LT083
Effective June 17, 2023, expires June 17, 2026

RECERTIFIED MAPPING SCIENTIST UAS

Jason Dolf, Certification #R017UAS
Effective April 19, 2023, expires April 19, 2028

ASPRS Certification validates your professional practice and experience. It differentiates you from others in the profession. For more information on the ASPRS Certification program: contact **certification@asprs.org,** visit **https://www.asprs.org/general/asprs-certification-program.html.**

asprs THE IMAGING & GEOSPATIAL INFORMATION SOCIETY

GIS Tips & Tricks

By Shira A. Ellenson, YoLani Martin, and Al Karlin, Ph.D., CMS-l, GISP

Making Your Maps more "Mappy Maps"

A cartographer acquaintance of mine once told me that when a map is on a coffee table and no one picks it up to examine, it is just a piece of paper. So, in an effort to help others learn tricks of the trade which draw attention to your map, to follow up on the past two columns on customizing text and colors on your maps, and to continue the theme of "never accepting the defaults", I asked two experienced map makers/cartographers to share some of the things they use to make their maps more "mappy". When pushing the art-envelope in cartography, attention to detail can be the difference between a map that sits on the coffee table, a good map, and great one.

Map Tip #1—Use Dropshadows to Make Polygons Pop Out of the Page

Take this simple polygon of Gates of the Arctic National Park in northern Alaska (Figure 1). This is the default line symbol and while it does delineate the feature, there is nothing special about the symbology to make a reader pick up the map. By customizing the line symbol, you achieve a look that enhances dimensionality to the area of interest rather than use the default symbology.
To make a more eye-popping boundary:

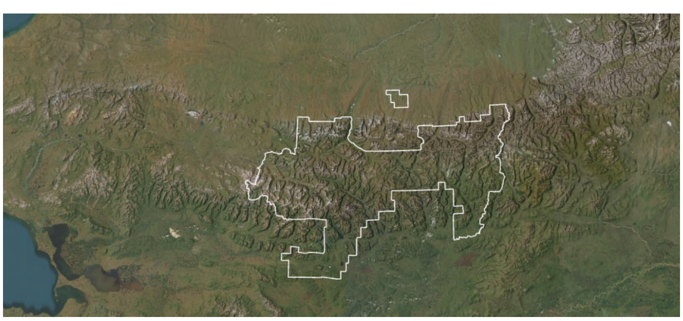

Figure 1. The default boundary polygon symbology for Gates of the Arctic National Park, Alaska.

1. Increase the stroke width and adjust it from "Solid stroke" to "Gradient stroke" (Figure 2)
2. Choose the same two colors as the "start" and "stop" scheme. With the first color selected, under Color Properties, reduce it to 100% transparency
3. Increase the offset to half of the stroke width so it renders on the outside of the polygon

The result is a drop shadow effect (Figure 3) that really makes your area of interest come to life.

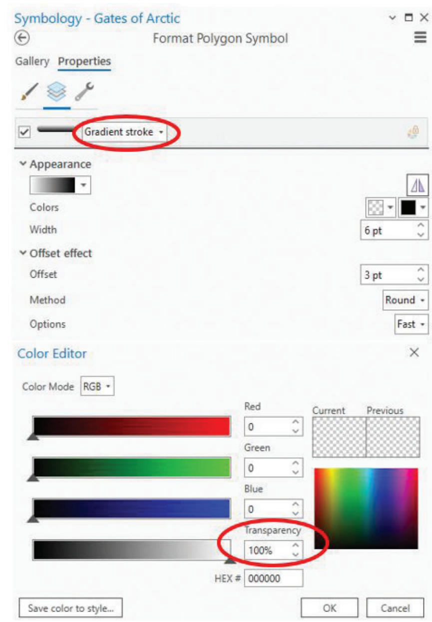

Figure 2. The Format Symbol | Properties dialog box showing the Gradient Fill properties.

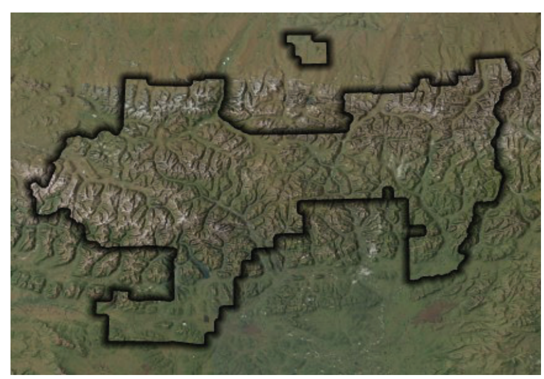

Figure 3. The Gates of the Arctic National Park boundary with customized dropdown shadow effect.

Map Tip #2—Use Enhanced Drop Shadows to Make Polygons Even More Effective

Take it one step further by using different blend modes! First, adjust the colors of the gradient stroke to go from 100% transparent white to white. Then add a solid fill of 40% gray.

Photogrammetric Engineering & Remote Sensing
Vol. 89, No. 10, October 2023, pp. 595-597.
0099-1112/22/595-597

doi: 10.14358/PERS.89.10.595

With the area of interest selected, under the "Feature Layer" tab on the ribbon (Figure 4), choose "Overlay" as the "Layer Blend". This blend mode boost contrasts by taking the lightness and darkness of the underlying layers and blending it with the top layer.

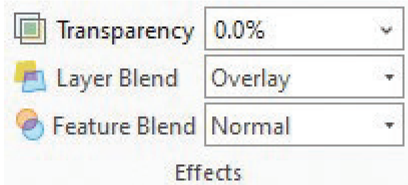

Figure 4. The "Effects" panel on the Feature Layer tab on the ribbon.

The result is a vibrant area of interest with a spotlight effect. The right blend mode is one that you think looks best, ex. Figure 5). Try playing around with different colors, sizes, offsets, and blend modes to achieve different effects!

Figure 5. Modifying the effects with a blend mode gives the area of interest a spotlight.

Map Tip #3—Make Water Look Like Water

Have you ever wanted to mimic the way light illuminates the surface of a waterbody? By using the same process of customizing symbology with a gradient, you can render basic polygons with an inner glow hack!

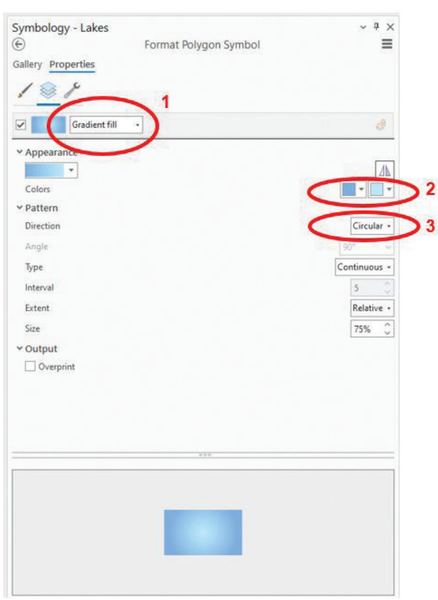

Figure 6. The Format Polygon Symbol | Properties menu showing customizations.

1. change your fill from "Solid" to "Gradient" (Figure 6), then
2. choose two colors that you would like to represent hydrology. I chose "Moorea Blue" (HEX #: 00A9E6) and "Sodalite Blue" (HEX #: BEE8FF) (remember the last month's color tips).
3. Under "Pattern", set the Direction to "Circular", and Type to "Continuous".

This ensures the gradient radiates in a circular pattern from the center of the polygon, giving the impression of concentric circles of varying colors. A continuous gradient allows for smooth transitions between colors.

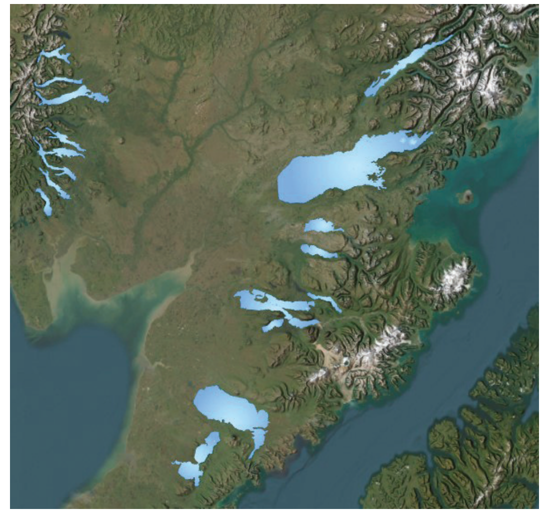

Figure 7. The results of customizing the lake polygon fill symbol with a custom gradient.

The result (Figure 7) is a soft illumination and radiant glow inviting us to jump in!

Map Tip #4—Context is Everything on a Locator Map

Shira was recently asked to make a map of Guam. When making the locator map, she realized the area she was working in would not provide much context until the map was really zoomed out to a VERY small scale. Here was an opportunity to use an orthographic projection, where Earth is depicted as a globe.

The only problem is that from this angle (Figure 8), Guam is out of range. To fix this, she had to make a custom coordinate system.

Figure 8. The "default" orthographic project of the earth does not show Guam, the area of interest for the project.

1. under Map Properties, search for "The World from Space" (Figure 9) and
2. set it as the Projected Coordinate System,
3. with the coordinate system selected, right click and select "Copy and Modify". This will prompt the "Modify Projected Coordinate System" window (Figure 10).
4. adjust the longitude and latitude so the area of interest is repositioned to your liking. Shira chose coordinates that would set Guam to be slightly off-center.

The result is a charming overview globe that gives better reference to the geographic area at large.

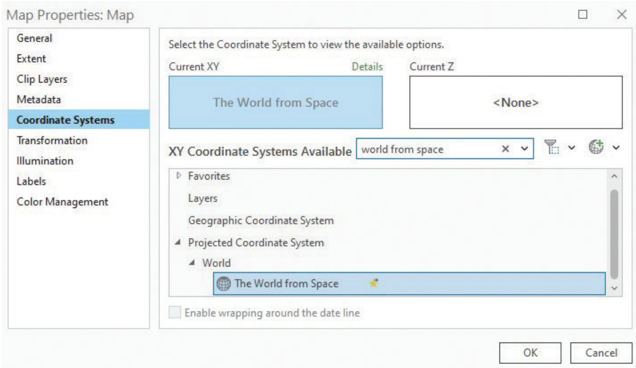

Figure 9. The Map Properties dialog is used to select "The World from Space" as the XY Coordinate System.

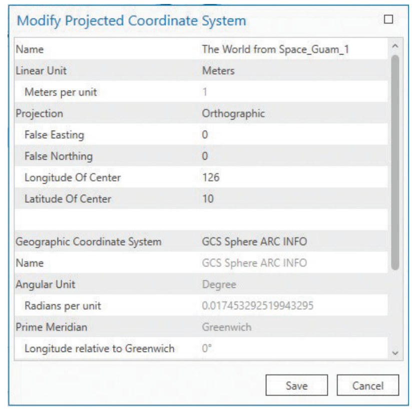

Figure 10. The Modify Project Coordinate System window is used to construct the custom coordinate system.

Figure 11. The custom coordinate system showing the area of interest (Guam) slightly off-center as determined by the cartographer.

Map Tip #5—Monochromatic Color Theory for Data Features

If stumped on what color to select for an individual feature layer's symbology, try using the lighter and darker variations of the feature's base color. This monochromatic approach can provide a variety of color selections and potentially provide more flexibility to a map's overall color scheme.

1. Select the base color that the data will be. In Figure 12 and 14, the base color is Rose Dust (RGB value 215, 158, 158).

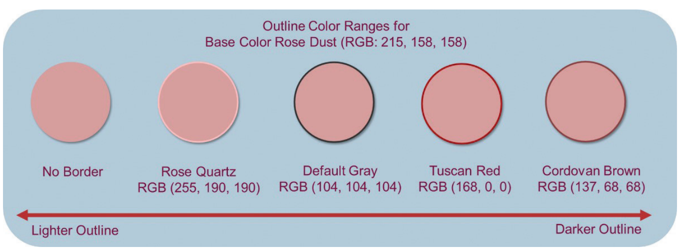

Figure 12. Outline color ranges surrounding the base color of Rose Dust (RGB value 215, 158, 158) where lighter variations of the base color stem to the left and darker variations stem to the right.

Use the color selector tool to find color variations of the base color (this will vary depending on the application being used). If your color selector tool provides default color blocks, focus in on one color range to for shading variations (Figure 13). If your color selector tool provides a color wheel/square (Figure 13), move the selection cursor up and to the left for lighter variations of the base color. Move the selection cursor down and to the right for darker variations of the color.

Figure 13. Left image of a color block selection tool from ArcMap Desktop. Right image of a color wheel/square tool from MediBang Paint.

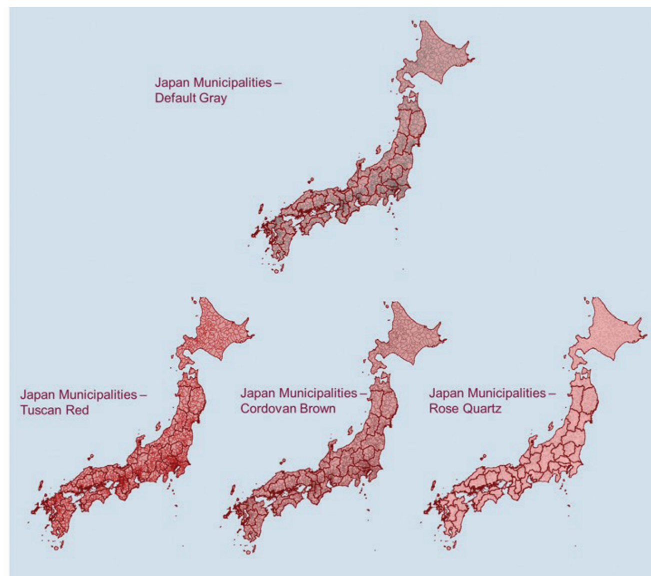

Figure 14. Maps of Japan's municipalities in various outline colors. The top map is in default gray (RGB value 104, 104, 104); bottom left map is in Tuscan Red (RGB value 168, 0, 0); bottom center map is in Cordovan Brown (137, 68, 68); bottom right map is in Rose Quartz (255, 190, 190).

Experiment with the color variations on the data features. In Figure 14, the top map of Japan has a default gray outline surrounding the municipalities feature. Below this, the color variations stemming from the municipalities feature's base color are applied to the outline.

This is a simple trick that can give your data visualizations an extra pop of character or double check if a visualization is accessible for an audience.

Send your questions, comments, and tips to GISTT@ASPRS.org.

Shira Ellenson is a Senior Geospatial Analyst with Dewberry's Anchorage, AK office. She specializes in remote sensing and cartography. YoLani Martin is a Geospatial Analyst with Dewberry's Fairfax, VA office. She is a resource for open source tools and Python scripting. Al Karlin, Ph.D., CMS-L, GISP is with Dewberry's Geospatial and Technology Services group in Tampa, FL. As a senior geospatial scientist, Al works with all aspects of Lidar, remote sensing, photogrammetry, and GIS-related projects.

The layman's perspective on technical theory and practical applications of mapping and GIS

MAPPING MATTERS

YOUR QUESTIONS ANSWERED

by Qassim Abdullah, Ph.D., PLS, CP
Woolpert Vice President and Chief Scientist

- **Have you ever wondered about what can and can't be achieved with geospatial technologies and processes?**
- **Have you been intimidated by formulas or equations in scientific journal articles and published reports?**
- **Would you like to understand the geospatial industry in layman's terms?**
- **Do you have a challenging technical question that no one you know can answer?**

If you answered "YES" to any of these questions, then you need to read Dr. Qassim Abdullah's column, Mapping Matters.

In it, he answers all geospatial questions—no matter how challenging—and offers accessible solutions.

Send your questions to Mapping_Matters@asprs.org

To browse previous articles of Mapping Matters, visit http://www.asprs.org/Mapping-Matters.html

"Your mapping matters publications have helped us a lot in refining our knowledge on the world of Photogrammetry. I always admire what you are doing to the science of Photogrammetry. Thank You Very much! the world wants more of enthusiast scientists like you."

"I read through your comments and calculations twice. It is very clear understandable. I am Honored there are experienced professionals like you, willing to help fellow members and promote knowledge in the Geo-Spatial Sciences."

YOUR COMPANION TO SUCCESS

ASPRS APPROVES EDITION 2 OF THE ASPRS POSITIONAL ACCURACY STANDARDS FOR DIGITAL GEOSPATIAL DATA

The American Society for Photogrammetry and Remote Sensing (ASPRS) is pleased to announce approval of the Positional Accuracy Standards for Geospatial Data, Edition 2, Version 1.0.

Edition 2, Version 1.0. includes Addendum I: General Best Practices and Guidelines and Addendum II: Best Practices and Guidelines for Field Surveying of Ground Control and Checkpoints. Modifications implemented in Edition 2 respond to evolving technologies and industry needs. The new edition was drafted by ASPRS subject matter experts representing public, private, and academic sectors. Public review was conducted from February 8 – April 30, 2023. Comments were incorporated into the final version adopted on August 23, 2023.

“The new edition of these standards will have a positive impact on our geospatial capabilities and all who benefit from these services here in the United States of America and worldwide for years to come, it is a historical moment that we should all be proud of,” said Dr. Qassim Abdullah, Vice President and Chief Scientist of Woolpert, who led the ASPRS Positional Accuracy Standards Working Group. “We are fortunate to have among our members such talented and willing volunteers who worked hard during the last two years to update this important Standard,” said Lorraine Amenda, ASPRS President.

As the USGS Lidar Base Specifications is well aligned with the ASPRS accuracy standards, users of the 3DEP program will reap the benefits from the modifications introduced in Edition 2. “As our 3DEP Lidar Base Specification is closely aligned with the ASPRS standards, we welcome these updates to the standards introduced in the Second Edition. We hope these updates bring even more clarity to an already well adopted standard on acquiring geospatial data,” said Dr. Michael Tischler, Director, USGS National Geospatial Program.

The most significant changes introduced in this 2nd Edition of the ASPRS Positional Accuracy Standards for Digital Geospatial Data include:

1. Elimination of references to the 95% confidence level as an accuracy measure.
2. Relaxation of the accuracy requirement for ground control and checkpoints.
3. Consideration of survey checkpoint accuracy when computing final product accuracy.
4. Removal of the pass/fail requirement for Vegetated Vertical Accuracy (VVA) for lidar data.
5. Increase the minimum number of checkpoints required for product accuracy assessment from twenty (20) to thirty (30).
6. Limiting the maximum number of checkpoints for accuracy assessment to 120 for large project.

7. Introduction of a new term, “three-dimensional positional accuracy.”
8. Addition of Guidelines and Best Practices Addendums for:
   a. General Guidelines and Best Practices
   b. Field Surveying of Ground Control and Checkpoints
   c. Mapping with Photogrammetry
   d. Mapping with Lidar
   e. Mapping with UAS

There are also three additional Addendums listed in the Table of Contents:

- Addendum III: Best Practices and Guidelines for Mapping with Photogrammetry
- Addendum IV: Best Practices and Guidelines for Mapping with Lidar
- Addendum V: Best Practices and Guidelines for Mapping with UAS

These three Addendums will be available for public comment in the coming weeks and will be added to Edition 2, Version 2.0, which ASPRS anticipates approving in late Fall 2023.

The significant changes in Edition 2 are summarized in the Foreword. To download the document, visit https://publicdocuments.asprs.org/PositionalAccuracyStd-Ed2-V1.

CALL FOR PARTICIPATION

NSRS Modernization Working Group

The Photogrammetric Applications Division of ASPRS is seeking interested community members to engage in the **NSRS Modernization Working Group**.

The National Geodetic Survey is replacing the NAD 83 reference frame and the NAVD 88 datum towards improving the National Spatial Reference System. With these changes, it is essential that the photogrammetry and remote sensing community be prepared to integrate the new reference frames into products and workflows. The NSRS Modernization Working Group seeks to develop and implement plans to support the ASPRS community in this transition.

If you are interested in participating in this working group, please reach out to Dr. Qassim Abdullah Qassim.Abdullah@Woolpert.com or Dr. Ben Wilkinson benew@ufl.edu

High-Definition Roads Mapping Working Group

The Photogrammetric Applications Division of ASPRS is seeking interested community members to engage in the **HD Roads Mapping Working Group**.

As the development of self-driving cars continues to progress, most automotive manufacturers have recognized the need for highly defined, precise, and accurate geospatial products to support autonomous navigation and steering. These high-definition maps are or can be provided by the ASPRS community and related industry. This working group seeks to engage industry and agencies associated with self-driving cars to identify critical geospatial components, develop national specifications, and to support product generation and standardization.

If you are interested in participating in this working group, please reach out to Dr. Qassim Abdullah Qassim.Abdullah@Woolpert.com or Dr. Ben Wilkinson benew@ufl.edu.

ASPRS Directory

Membership/*PE&RS* Subscription
office@asprs.org

Conferences
programs@asprs.org

Certification
applications@asprs.org

Calendar
calendar@asprs.org

ASPRS Bookstore
office@asprs.org

ASPRS Foundation
foundation@asprs.org

ASPRS Board of Directors
asprsboard@asprs.org

Student Advisory Council
sac@asprs.org

Early-Career Professionals Council
ecpc@asprs.org

Region Officers Council
roc@asprs.org

Sustaining Members Council
smc@asprs.org

Technical Division Directors Council
tddc@asprs.org

PO Box 14713, Baton Rouge, LA 70898 | 225-408-4747, 225-408-4422 (fax), www.asprs.org

ASPRS Workshop Series

It’s not too late to earn Professional Development Hours

Miss one of our Live Online Workshops? You can purchase the workshops now and watch when you are ready!

Check out the workshops offered by visiting **https://asprs.prolearn.io/catalog**

Ad Index

Mapping Lotus Wetland Distribution with the Phenology Normalized Lotus Index Using SAR Time-Series Imagery and the Phenology-Based Method

Sheng Wang, Taixia Wu, and Qiang Shen

Abstract

Lotus wetland is a type of wetland that can efficiently purify water. Therefore, rapid and accurate remote sensing monitoring of the distribution of lotus wetland has great significance to their conservation and the promotion of a sustainable and healthy development of ecosystems. The phenology-based method has proven effective in mapping some different types of wetlands. However, because of the serious absence of remote sensing data caused by cloud coverage and the differences in the phenological rhythms of lotus wetlands in different areas, achieving high-precision mapping of different regions using a unified approach is a challenge. To address the issue, this article proposes a Phenology Normalized Lotus Index (PNLI) model that combines SAR time-series imagery and the phenology-based method. The results of this study demonstrate that the PNLI model shows good applicability in different areas and has high mapping accuracy. The model can map the lotus wetland distribution in large areas quickly and simultaneously with high precision.

Introduction

An important part of freshwater ecosystems, wetlands have characteristics of both terrestrial and freshwater ecosystems and promote a balance between ecosystems (Colin *et al.* 2018; Seifollahi-Aghmiuni *et al.* 2019). It is renowned for its exceptional purification capabilities, earning it the epithet "the kidney of the earth" (Waltham *et al.* 2019; Kaushalya 2020). Among various types of wetlands, lotus wetland holds particular importance, as it plays a unique role in reducing waterborne pollutants, such as chemical oxygen demand (COD), biochemical oxygen demand (BOD), and ammoniacal nitrogen (Kanabkaew and Puetpaiboon 2004; Jou *et al.* 2008; Abd Rasid *et al.* 2019). Presently, many wetlands in China and other developing countries experience pollution issues, including elevated levels of COD (Chi *et al.* 2020), BOD (Song *et al.* 2006), and ammonia (Teng *et al.* 2017). However, lotus plants in lotus wetlands effectively mitigate these pollutants (Abd Rasid *et al.* 2019). Therefore, obtaining accurate distribution information on lotus wetland vegetation in both time and space holds significant ecological and theoretical significance, as it aids in unraveling the response mechanisms to water environmental factors (Jiang and Xu 2019) while also providing substantial practical value in water pollution control (De Groot *et al.* 2018). Satellite remote sensing, a rapidly evolving technology over the past three decades, has long been extensively employed for mapping vegetation distribution (Skriver 2007; Gholizadeh and Melesse 2017). Consequently, satellite remote sensing technology offers the potential to rapidly and comprehensively obtain distribution information for lotus wetlands (Fournier *et al.* 2007; Colvin *et al.* 2019).

The phenology-based method offers a valuable approach for mapping the distribution of wetland plants utilizing satellite remote sensing technology. Due to the distinct remote sensing characteristics exhibited by different wetland plant species during phenological stages, this method proves to be feasible for accurately delineating the coverage area of individual wetland vegetation (Wessels *et al.* 2011). By employing multi-temporal optical remote sensing imagery, the phenology-based method generates temporal profiles of remote sensing parameters, enabling the identification of phenological time nodes for each plant species within specific phenological periods. These remote sensing parameters serve as phenological features that, when combined with classification models, facilitate the extraction and mapping of vegetation areas (Dannenberg *et al.* 2020). Notably, previous studies have demonstrated advancements in plant extraction methods based on phenological characteristics, often employing closely related indicators, such as the normalized difference vegetation index (NDVI) or the enhanced vegetation index (EVI), indicative of plant growth conditions (Zhang *et al.* 2022). For example, researchers successfully differentiated between corn, soybean, and tobacco fields in large commercial farms in Africa by utilizing time-series MODIS imagery and NDVI values at phenological time nodes as phenological features (Maguranyanga *et al.* 2015). Another study combined time-series MODIS imagery with ground data to confirm the significant discriminating capability of NDVI-based phenological feature information in distinguishing cotton from corn and sorghum within agricultural landscapes (Sibanda *et al.* 2010). MODIS imagery is a composite observation of Terra and Aqua satellites, providing medium-resolution data. These synthetic satellites enable repeated observations of the entire Earth's surface within 1–2 days, offering improved temporal resolution accuracy. However, the spatial resolution accuracy of MODIS imagery is limited, with the highest accuracy for plant phenology monitoring being 250 m. Consequently, many scholars opt for high-spatial-resolution remote sensing image data to map plant distributions using phenology-based methods (Xu *et al.* 2018). For example, Chen *et al.* (2014) incorporated the time information of phenological nodes of plants in their study area and employed NDVI and EVI values extracted from *Landsat 8* imagery as phenological features. By combining these features with the maximum likelihood method, they successfully extracted wheat planting areas, demonstrating that EVI combined with the EVI maximum likelihood method (EVI_{ML}) outperformed NDVI combined with the maximum likelihood method ($NDVI_{ML}$), achieving mapping accuracy exceeding 85% (Chen *et al.* 2014). Zhang *et al.* (2018) employed the *Landsat 8* time-series curve

Sheng Wang, Taixia Wu, and Qiang Shen are with the School of Earth Sciences and Engineering, Hohai University, Nanjing, China.

Corresponding author: Sheng Wang, wangsh12@hhu.edu.cn

Contributed by Ravi Dwivedi, February 13, 2023 (sent for review May 30, 2023; reviewed by Ajai Ajai, Jai Jai Garg).

Photogrammetric Engineering & Remote Sensing
Vol. 89, No. 10, October 2023, pp. 601–611.
0099-1112/22/601–611

doi: 10.14358/PERS.23-00012R2

PEER-REVIEWED CONTENT
IS ONLY AVAILABLE TO
ASPRS MEMBERS AND SUBSCRIBERS

FOR MORE INFORMATION VISIT
MY.ASPRS.ORG

PEER-REVIEWED CONTENT
IS ONLY AVAILABLE TO
ASPRS MEMBERS AND SUBSCRIBERS

FOR MORE INFORMATION VISIT
MY.ASPRS.ORG

PEER-REVIEWED CONTENT
IS ONLY AVAILABLE TO
ASPRS MEMBERS AND SUBSCRIBERS

FOR MORE INFORMATION VISIT
MY.ASPRS.ORG

PEER-REVIEWED CONTENT
IS ONLY AVAILABLE TO
ASPRS MEMBERS AND SUBSCRIBERS

FOR MORE INFORMATION VISIT
MY.ASPRS.ORG

PEER-REVIEWED CONTENT
IS ONLY AVAILABLE TO
ASPRS MEMBERS AND SUBSCRIBERS

FOR MORE INFORMATION VISIT
MY.ASPRS.ORG

PEER-REVIEWED CONTENT
IS ONLY AVAILABLE TO
ASPRS MEMBERS AND SUBSCRIBERS

FOR MORE INFORMATION VISIT
MY.ASPRS.ORG

PEER-REVIEWED CONTENT
IS ONLY AVAILABLE TO
ASPRS MEMBERS AND SUBSCRIBERS

FOR MORE INFORMATION VISIT
MY.ASPRS.ORG

PEER-REVIEWED CONTENT
IS ONLY AVAILABLE TO
ASPRS MEMBERS AND SUBSCRIBERS

FOR MORE INFORMATION VISIT
MY.ASPRS.ORG

PEER-REVIEWED CONTENT
IS ONLY AVAILABLE TO
ASPRS MEMBERS AND SUBSCRIBERS

FOR MORE INFORMATION VISIT
MY.ASPRS.ORG

Seifollahi-Aghmiuni, S., Z. Kalantari, M. Land and G. Destouni. 2019. Change drivers and impacts in Arctic wetland landscapes—Literature review and gap analysis. *Water* 11(4):722.

Sibanda, M., A. Murwira and F. Baudron. 2010. *Evaluating the Relative Contribution of Changing Farming Methods to Habitat Loss in the Mid-Zambezi Valley*. Ph.D. dissertation, University of Zimbabwe.

Skriver, H. 2007. Signatures of polarimetric parameters and their implications on land cover classification. Pages 4195–4198 in *IEEE International Geoscience and Remote Sensing Symposium*, held in Barcelona, Spain, 23–28 July 2007. New York: IEEE.

Song, Z., Z. Zheng, J. Li, X. Sun, X. Han, W. Wang and M. Xu. 2006. Seasonal and annual performance of a full-scale constructed wetland system for sewage treatment in China. *Ecological Engineering* 26(3):272–282.

Teng, X., Q. Hu, L. Zhang , J. Qi, J. Shi, H. Xie, H. Gao and X. Yao. 2017 Identification of major sources of atmospheric NH_3 in an urban environment in northern China during wintertime. *Environmental Science and Technology* 51(12):6839–6848.

Waltham, N. J., D. Burrows, C. Wegscheidl, C. Buelow, M. Ronan, N. Connolly, G. Paul, M. A. Donna, C. Colin and S. Marcus. 2019 Lost floodplain wetland environments and efforts to restore connectivity, habitat, and water quality settings on the Great Barrier Reef. *Frontiers in Marine Science* 6:71.

Wessels, K., K. Steenkamp, G. Von Maltitz and S. Archibald. 2011. Remotely sensed vegetation phenology for describing and predicting the biomes of South Africa. *Applied Vegetation Science* 14(1):49–66.

Xie, F., D. Chen, D. J. Meligrana and W. Ren. 2013. Selecting key features for remote sensing classification by using decision-theoretic rough set model. *Photogrammetric Engineering and Remote Sensing* 79(9):787–797.

Xu, P., Z. Niu and P. Tang. 2018. Comparison and assessment of NDVI time series for seasonal wetland classification. *International Journal of Digital Earth* 11(11):1103–1131.

Zhang, B., X. Liu, M. Liu and Y. Meng. 2018. Detection of rice phenological variations under heavy metal stress by means of blended Landsat and MODIS image time series. *Remote Sensing* 11(1):13.

Zhang, H., X. Wang and D. Peng. 2022. Evaluation of urban vegetation phenology using 250 m MODIS vegetation indices. *Photogrammetric Engineering and Remote Sensing* 88(7):461–467.

Zhang, M., F. Chen, D. Liang, B. Tian and A. Yang. 2020. Use of Sentinel-1 GRD SAR imagery to delineate flood extent in Pakistan. *Sustainability* 12(14):5784.

In-Press Articles

Identification of Critical Urban Clusters for Placating Urban Heat Island Effects over Fast-Growing Tropical City Regions: Estimating the Contribution of Different City Sizes in Escalating UHI Intensity. Kanaya Dutta, Debolina Basu, and Sonam Agrawal.

A Novel Object Detection Method for Solid Waste Incorporating a Weighted Deformable Convolution. Xiong Xu, Tao Cheng, Beibei Zhao, Chao Wang, Xiaohua Tong, Yongjiu Feng, Huan Xie, and Yanmin Jin.

An Integrated Approach for Wildfire Photography Telemetry using WRF Numerical Forecast Products. Ling Tan and Xuelan Ma.

A Powerful Correspondence Selection Method for Point Cloud Registration Based on Machine Learning. Wuyong Tao, Dong Xu, Xijiang Chen, and Ge Tan.

Self-Calibration of the Stereo Vision System on the Chang’E-5 Probe Based on Images and Robot Arm Footprints. Shuo Zhang, Yanhong Zheng, Liping Chen, Youqing Ma, Bo Hu, Zheng Gu, Xiangjin Deng, and Shaochuang Liu.

Combination of Terrestrial Laser Scanning and Unmanned Aerial Vehicle Photogrammetry for Heritage Building Information Modeling: A Case Study of Tarsus St. Paul Church. Şafak Fidan, Ali Ulvi, Abdurahman Yasin Yiğit, Seda Nur Gamze Hamal, and Murat Yakar.

IMU and Bluetooth Data Fusion to Achieve Submeter Position Accuracy in Indoor Positioning. Ugur Acar.

Rice Identification Under Complex Surface Conditions with CNN and Integrated Remote Sensing Spectral-Temporal-Spatial Features. Tianjiao Liu, Jiankui Chen, Li Zhang, and Dong Li.

Call for *PE&RS* Special Issue Submissions

Ushering a New Era of Hyperspectral Remote Sensing to Advance Remote Sensing Science in the Twenty-first Century

Great advances are taking place in remote sensing with the advent of new generation of hyperspectral sensors. These include data from, already in orbit sensors such as: 1. Germany's Deutsches Zentrum fur Luftund Raumfahrt (DLR's) Earth Sensing Imaging Spectrometer (DESIS) sensor onboard the International Space Station (ISS), 2. Italian Space Agency's (ASI's) PRISMA (Hyperspectral Precursor of the Application Mission), and 3. Germany's DLR's Environmental Mapping and Analysis Program (EnMAP). Further, Planet Labs PBC recently announced the launch of two hyperspectral sensors called Tanager in 2023. NASA is planning for the hyperspectral sensor Surface Biology and Geology (SBG) to be launched in the coming years. Further, we already have over 70,000 hyperspectral images of the world acquired from NASA's Earth Observing-1 (EO-1) Hyperion that are freely available to anyone from the U.S. Geological Survey's data archives. These suites of sensors acquire data in 200 plus hyperspectral narrowbands (HNBs) in 2.55 to 12 nm bandwidth, either in 400-1000 or 400-2500 nm spectral range with SBG also acquiring data in the thermal range. In addition, Landsat-NEXT is planning a constellation of 3 satellites each carrying 26 bands in the 400-12,000 nm wavelength range. HNBs provide data as "spectral signatures" in stark contrast to "a few data points along the spectrum" provided by multispectral broadbands (MBBs) such as the Landsat satellite series.

The goal of this special issue is to seek scientific papers that perform research utilizing data from these new generation hyperspectral narrowband (HNB) sensors for a wide array of science applications and compare them with the performance of the multispectral broadband (MBB) sensors such as Landsat, Sentinels, MODIS, IRS, SPOT, and a host of others.

Papers on the following topics are of particular interest:

1. Methods and techniques of understanding, processing, and computing hyperspectral data with specific emphasis on machine learning, deep learning, artificial intelligence (ML/DL/AI), and cloud computing.
2. Issues of hyperspectral data volumes, data redundancy, and overcoming Hughes' phenomenon.
3. Building hyperspectral libraries for purposes of creating reference training, testing, and validation data.
4. Utilizing time-series multispectral data and hyperspectral data over many years to build data cubes and apply advanced computational methods of ML/DL/AI methods and approaches on the cloud.
5. Discussions of hyperspectral data analysis techniques like full spectral analysis versus optimal band analysis.
6. Developing hyperspectral vegetation indices (HVIs) for targeted applications to model and map plant biophysical (e.g., Yield, biomass, leaf area index), biochemical (e.g., Nitrogen, anthocyanins, carotenoids), plant health/stress, and plant structural quantities.
7. Classification of complex vegetation and crop types/species using HNBs and HVIs and comparing them with the performance of multispectral broadband data.

All submissions will be peer-reviewed in line with *PE&RS* policy. Because of page limits, not all submissions recommended for acceptance by the review panel may be included in the special issue. Under this circumstance, the guest editors will select the most relevant papers for inclusion in the special issue. Authors must prepare manuscripts according to the *PE&RS* Instructions to Authors, published in each issue of *PE&RS* and also available on the ASPRS website, https://www.asprs.org/asprs-publications/pers/manuscript-submission.

Special Issue Editors

Dr. Prasad S. Thenkabail, pthenkabail@usgs.gov, thenkabail@gmail.com
Senior Scientist (ST), USGS, Flagstaff, Arizona

Dr. Itiya Aneece, ianeece@usgs.gov
USGS, Flagstaff, Arizona

Dr. Pardhasaradhi Teluguntla, pteluguntla@usgs.gov
USGS, Flagstaff, Arizona

Important Dates

Manuscripts Due — December 15, 2023

Final Papers Due — May 1, 2024

Tentative Publication Date — 2024

Please submit your manuscript —
www.editorialmanager.com/asprs-pers/
select "Hyperspectral Remote Sensing"

The FABDEM Outperforms the Global DEMs in Representing Bare Terrain Heights

Nahed Osama, Zhenfeng Shao, and Mohamed Freeshah

Abstract

Many remote sensing and geoscience applications require a high-precision terrain model. In 2022, the Forest And Buildings removed Copernicus digital elevation model (FABDEM) was released, in which trees and buildings were removed at a 30 m resolution. Therefore, it was necessary to make a comprehensive evaluation of this model. This research aims to perform a qualitative and quantitative analysis of FABDEM in comparison with the commonly used global DEMs. We investigated the effect of the terrain slope, aspect, roughness, and land cover types in causing errors in the topographic representation of all DEMs. The FABDEM had the highest overall vertical accuracy of 5.56 m. It was the best DEM in representing the terrain roughness. The FABDEM and Copernicus DEM were equally influenced by the slopes more than the other models and had the worst accuracy of slope representation. In the tree, built, and flooded vegetation areas of the FABDEM, the mean errors in elevation have been reduced by approximately 3.34 m, 1.26 m and 1.55 m, respectively. Based on Welch's t-test, there was no significant difference between FABDEM and Copernicus DEM elevations. However, the slight improvements in the FABDEM make it the best filtered DEM to represent the terrain heights over different land cover types.

Introduction

Digital elevation models (DEMs) are considered the core spatial data set required for a variety of applications such as hydrological research (Chu and Lindenschmidt 2017), terrain analysis (Osama *et al.* 2021), soil science (Park *et al.* 2001), ecology (Amatulli *et al.* 2018; Moore *et al.* 1991), glaciology (Rentsch *et al.* 1990; Wang and Kääb 2015), and volcanology (Grosse *et al.* 2012; Kubanek *et al.* 2021). DEMs have existed at a global or near-global scale with 1 arc second grid spacing based on geo-rectified space data acquired from several sensors such as optical, near-infrared, and radar sensors. In 2000, some satellites have been launched to collect (30 m–90 m) resolution elevation data for the globe such as the Shuttle Radar Topography Mission (SRTM) and the Advanced Spaceborne Thermal Emission and Reflection Radiometer (ASTER) mission (Mukherjee *et al.* 2012). Since then, the DEMs collected by them are freely available for public use in various resolutions. From 2006 to 2011 the Japanese Aerospace Exploration Agency (JAXA) has used the Advanced Land Observing Satellite (ALOS) releases to produce the world three-dimensional (3D) topographic data, the most precise DEM at that time, with a horizontal resolution of 30 meter. In 2020, National Aeronautics and Space Administration (NASA) reprocessed SRTM by an optimized hybrid processing approach based on expanding spatial coverage and minimizing data voids. The voids have been filled with a variety of data sets including ASTER, ALOS, United States Geological Survey (USGS) national elevation data set, and Canada and Alaska DEMs. Meanwhile, ground control points and ICESat data were used for vertical and tilt adjustments (NASA JPL 2020). In December 2020, the European Space Agency (ESA) made the 30-meter resolution Copernicus DEM available for free (ESA 2020). Since then, some studies were performed to investigate the Copernicus DEM accuracy and compare its errors with the previous global DEMs errors (Guth and Geoffroy 2021).

DEMs are subjected to several sources of errors during the data processing due to the oldness of data, low density of observation, filtering or interpolation, and resampling errors. In literature, SRTM and Terra Advanced Spaceborne Thermal Emission and Reflection Radiometer (ASTER) DEMs exhibited large vertical errors, especially over complex topography, and they have defects in relatively flat terrain where they cannot deal with microtopographic variations (Chu and Lindenschmidt 2017; Gallien *et al.* 2011). Relative and absolute elevation errors for the SRTM mission were defined as 6 m and 16 m, respectively (Rabus *et al.* 2003). Nevertheless, recent studies have shown that the accuracy of the SRTM DEM is still acceptable in many applications (Liu *et al.* 2020). On this basis, several studies were based on merging different elevation data sets to improve DEMs' accuracy and eliminate biases of vegetation and man-made features, such as buildings and other types of infrastructure (Baugh *et al.* 2013; O'Loughlin *et al.* 2016; Robinson *et al.* 2014; Yamazaki *et al.* 2017; Yue *et al.* 2017). Even so, the derived versions have shown multiple errors in the vertical values much larger than those acceptable for several applications when they have been used widely (Mukherjee *et al.* 2012).

Over years, the vertical accuracies of the SRTM DEM, ASTER DEM, and the other global DEMs have been investigated by remote sensing community. The SRTM showed a better vertical accuracy than a 1:50 000 topographic maps within the range of 8 m and 20 m (Jarvis *et al.* 2004). The vertical accuracies of ASTER DEM in Spain and Turkey were 4 m and 8 m, respectively (Sefercik 2012). In China, both ASTER DEM and SRTM DEM vertical accuracies have been investigated in two different areas, SRTM DEM showed root-mean-square error (RMSE) values of 2.38 m and 4.43 m, and ASTER DEM showed RMSE values of 6.98 m and 4.83 m (Du *et al.* 2012). ALOS 3D world DEM (AW3D30) accuracy has been tested among seven global DEMs including ASTER and SRTM DEMs. The results showed that ALOS DEM had the greatest vertical accuracy in the selected regions (Liu *et al.* 2019). While in another similar studies AW3D30 DEM was also superior to ASTER DEM and SRTM DEM (González-Moradas and Viveen 2020). Over the five available global one arc second DEMs, (ASTER, SRTM, ALOS, NASA, and Copernicus), evaluated in eight high-relief areas through wide-distributed lidar point clouds and ICESat-2 data. The Copernicus DEM showed superiority in elevation accuracy in slopes (i.e., steep and gentle lands) and in different vegetation regions, over the abovementioned global DEMs (Guth and Geoffroy 2021). Since the DEMs have differences in strategy, models, data collection time, mission, and geographical extent, the

Nahed Osama and Zhenfeng Shao are with the State Key Laboratory of Information Engineering in Surveying, Mapping and Remote Sensing, Wuhan University, Wuhan 430079, China.

Zhenfeng Shao is also with Hubei Luojia Laboratory, Wuhan, China.

Mohamed Freeshah is with the School of Geodesy and Geomatics, Wuhan University, 129 Luyuo Road, Wuhan 430079, China and the Department of Geomatics Engineering, Faculty of Engineering at Shoubra, Benha University, Cairo 11629, Egypt.

Corresponding author: Mohamed Freeshah, mohamedfreeshah@whu.edu.cn

Contributed by Prasad S. Thenkabail, April 7, 2023 (sent for review May 8, 2023; reviewed by Fanar M. Abed, Zhaojin Li).

Photogrammetric Engineering & Remote Sensing
Vol. 89, No. 10, October 2023, pp. 613–624.
0099-1112/22/613–624

doi: 10.14358/PERS.23-00026R2

PEER-REVIEWED CONTENT
IS ONLY AVAILABLE TO
ASPRS MEMBERS AND SUBSCRIBERS

FOR MORE INFORMATION VISIT
MY.ASPRS.ORG

PEER-REVIEWED CONTENT
IS ONLY AVAILABLE TO
ASPRS MEMBERS AND SUBSCRIBERS

FOR MORE INFORMATION VISIT
MY.ASPRS.ORG

PEER-REVIEWED CONTENT IS ONLY AVAILABLE TO ASPRS MEMBERS AND SUBSCRIBERS

FOR MORE INFORMATION VISIT MY.ASPRS.ORG

**PEER-REVIEWED CONTENT
IS ONLY AVAILABLE TO
ASPRS MEMBERS AND SUBSCRIBERS**

**FOR MORE INFORMATION VISIT
MY.ASPRS.ORG**

PEER-REVIEWED CONTENT
IS ONLY AVAILABLE TO
ASPRS MEMBERS AND SUBSCRIBERS

FOR MORE INFORMATION VISIT
MY.ASPRS.ORG

PEER-REVIEWED CONTENT
IS ONLY AVAILABLE TO
ASPRS MEMBERS AND SUBSCRIBERS

FOR MORE INFORMATION VISIT
MY.ASPRS.ORG

PEER-REVIEWED CONTENT
IS ONLY AVAILABLE TO
ASPRS MEMBERS AND SUBSCRIBERS

FOR MORE INFORMATION VISIT
MY.ASPRS.ORG

PEER-REVIEWED CONTENT IS ONLY AVAILABLE TO ASPRS MEMBERS AND SUBSCRIBERS

FOR MORE INFORMATION VISIT MY.ASPRS.ORG

PEER-REVIEWED CONTENT
IS ONLY AVAILABLE TO
ASPRS MEMBERS AND SUBSCRIBERS

FOR MORE INFORMATION VISIT
MY.ASPRS.ORG

PEER-REVIEWED CONTENT
IS ONLY AVAILABLE TO
ASPRS MEMBERS AND SUBSCRIBERS

FOR MORE INFORMATION VISIT
MY.ASPRS.ORG

Evaluating Surface Mesh Reconstruction Using Real Data

Yanis Marchand, Laurent Caraffa, Raphael Sulzer, Emmanuel Clédat, and Bruno Vallet

Abstract

Surface reconstruction has been studied thoroughly, but very little work has been done to address its evaluation. In this article, we propose new visibility-based metrics to assess the completeness and accuracy of three-dimensional meshes based on a point cloud of higher accuracy than the one from which the reconstruction has been computed. We use the position from which each high-quality point has been acquired to compute the corresponding ray of free space. Based on the intersections between each ray and the reconstructed surface, our metrics allow evaluating both the global coherency of the reconstruction and the accuracy at close range. We validate this evaluation protocol by surveying several open-source algorithms as well as a piece of licensed software on three data sets. The results confirm the relevance of assessi ng local and global accuracy separately since algorithms sometimes fail at guaranteeing both simultaneously. In addition, algorithms making use of sensor positions perform better than the ones relying only on points and normals, indicating a potentially significant added value of this piece of information. Our implementation is available at https://github.com/umrlastig/SurfaceReconEval.

Introduction

Surface reconstruction is the task of producing a continuous digital representation of a real surface of which discrete information has been acquired. This information may come straight from point clouds produced by a laser scanner. This includes time-of-flight (Lange and Seitz 2001) and structured-light (Geng 2011) devices as well as terrestrial and airborne lidar (Lohani and Ghosh 2017) that allow scanning large environments. Point clouds can also be produced from images using multi-view stereo (Furukawa and Hernández 2015) or structure from motion (Ozyesil *et al.* 2017).

This task has been extensively studied, and a large number of approaches have been proposed. In the section "Related Work," we provide a description of these state-of-the-art methods. However, very few articles address the evaluation of such a task. In real-case scenarios for which the goal is to produce a digital model of a real object or scene, there is no ground truth other than the real surface itself. It is thus impossible to directly compute the distance or the difference between a digital model and the ideal real surface. The only possible work-around is using synthetic data as in Marchand *et al.* (2021), where a realistic surface is chosen to be the ground truth and then virtually scanned in a way that simulates the defects of a real acquisition; the surface reconstruction algorithms to be evaluated are run on this virtual scan. This makes it more straightforward to compute metrics that assess the difference between the ground-truth model and the reconstructed ones. Another possibility for working with data from real scenes is to sample points from a reconstructed mesh, but this introduces a large bias, as methods producing the same features will be unfairly favored. Our work tackles the real-world case where we do not have access to such a synthetic ground truth. We call *real data* the data acquired in the physical world with real sensors. This includes lidar scans, images, RGB-D images, and so on. As is usually done to address this issue, we assess the reconstruction of real scenes from real data only based on other real data of significantly higher quality. Even though this idea is quite typical, the main contribution of this article lies in the way that we assess the difference between the reconstructed surface and the high-quality real data as inconsistencies, inspired by recent work on change detection (Xiao *et al.* 2015). The fundamental interest of this work is to propose metrics to assess the quality of reconstructions from low-quality real data based on high-quality data. Although it is possible to assess the quality of models visually, this raises several issues. First, it is a subjective comparison, and one might be tempted to favor their own or preferred method over others. Second, everyone has a different perception of visual quality, and we might not agree even without conflict of interest. Third, while it might sound reasonable to visually evaluate a few different models of a relatively small scene, it is very unlikely that one would be able to carry out a large-scale evaluation involving dozens of models representing large areas. Consequently, we believe that it is essential to find relevant metrics to assess surface reconstruction, and, in our opinion, current metrics are not entirely satisfying. As pointed out by Van Kreveld *et al.* (2013), there is a lack of ground truth and of benchmarks in the field of urban reconstruction. This article aims to tackle this problem. This endeavor is difficult for several reasons.

Limits in the Quality of the Ground Truth

The specificity of working with real data is the presence of noise in what we consider as the ground truth. In addition, real data are always sparse and incomplete, which means that we do not know the state of space (occupied by the object or empty) everywhere. This raises the question of how to assess pieces of reconstructed surface in unseen, unobserved regions.

Our contributions are twofold:

1. We propose a setting where the high-quality data used to compute metrics are significantly better than the low-quality data on which surface reconstruction is performed in three separate ways:
    a. Coverage: We use multiple data sources acquired from multiple points of view to ensure that the high-quality data have a significantly better coverage of the surface to reconstruct than the low-quality data.
    b. Density: We ensure that the density of the points in the high-quality data is significantly better than that of the low-quality data.
    c. Noise: We ensure that the noise level is lower in the high-quality data than in the low-quality data.
2. We propose metrics that penalize inconsistencies between the surface to be evaluated and the high-quality data: a piece of surface reconstructed within a volume unseen by the high-quality data will simply not be evaluated, as we have no information on it. This does not mean that we do not evaluate the hole-filling capacity of the evaluated methods. As the high-quality data have more coverage, we evaluate hole filling exactly where we have the data to do so.

Yanis Marchand, Laurent Caraffa, Raphael Sulzer, Emmanuel Clédat, and Bruno Vallet are with LASTIG, Univ Gustave Eiffel, IGN-ENSG, F-94160, Saint-Mande, France.

Corresponding author: Yanis Marchand (yanismarchan@gmail.com)

Contributed by Rongjun Qin, January 24, 2023 (sent for review January 29, 2023; reviewed by Shuang Song).

Photogrammetric Engineering & Remote Sensing
Vol. 89, No. 10, October 2023, pp. 625–638.
0099-1112/22/625–638

doi: 10.14358/PERS.23-00007R3

PEER-REVIEWED CONTENT
IS ONLY AVAILABLE TO
ASPRS MEMBERS AND SUBSCRIBERS

FOR MORE INFORMATION VISIT
MY.ASPRS.ORG

PEER-REVIEWED CONTENT
IS ONLY AVAILABLE TO
ASPRS MEMBERS AND SUBSCRIBERS

FOR MORE INFORMATION VISIT
MY.ASPRS.ORG

PEER-REVIEWED CONTENT
IS ONLY AVAILABLE TO
ASPRS MEMBERS AND SUBSCRIBERS

FOR MORE INFORMATION VISIT
MY.ASPRS.ORG

PEER-REVIEWED CONTENT
IS ONLY AVAILABLE TO
ASPRS MEMBERS AND SUBSCRIBERS

FOR MORE INFORMATION VISIT
MY.ASPRS.ORG

PEER-REVIEWED CONTENT
IS ONLY AVAILABLE TO
ASPRS MEMBERS AND SUBSCRIBERS

FOR MORE INFORMATION VISIT
MY.ASPRS.ORG

PEER-REVIEWED CONTENT
IS ONLY AVAILABLE TO
ASPRS MEMBERS AND SUBSCRIBERS

FOR MORE INFORMATION VISIT
MY.ASPRS.ORG

**PEER-REVIEWED CONTENT
IS ONLY AVAILABLE TO
ASPRS MEMBERS AND SUBSCRIBERS**

**FOR MORE INFORMATION VISIT
MY.ASPRS.ORG**

PEER-REVIEWED CONTENT
IS ONLY AVAILABLE TO
ASPRS MEMBERS AND SUBSCRIBERS

FOR MORE INFORMATION VISIT
MY.ASPRS.ORG

PEER-REVIEWED CONTENT
IS ONLY AVAILABLE TO
ASPRS MEMBERS AND SUBSCRIBERS

FOR MORE INFORMATION VISIT
MY.ASPRS.ORG

PEER-REVIEWED CONTENT
IS ONLY AVAILABLE TO
ASPRS MEMBERS AND SUBSCRIBERS

FOR MORE INFORMATION VISIT
MY.ASPRS.ORG

PEER-REVIEWED CONTENT
IS ONLY AVAILABLE TO
ASPRS MEMBERS AND SUBSCRIBERS

FOR MORE INFORMATION VISIT
MY.ASPRS.ORG

Different Urbanization Levels Lead to Divergent Responses of Spring Phenology

Chaoya Dang, Zhenfeng Shao, Xiao Huang, Gui Cheng, and Jiaxin Qian

Abstract

Urban vegetation phenology is important for understanding the relationship between human activities on urban ecosystems and carbon cycle. The relationship between urban and rural vegetation phenology and environmental and meteorological factors were studied across urban-rural gradients. However, the relationship of intra-urban urbanization intensity (UI) gradients on vegetation at the start of season (SOS) is unclear. Here, we used remote sensing data to quantitatively assess the relationship of vegetation SOS to UI gradients at mid-high latitudes in the northern hemisphere. The results showed that urban area vegetation SOS widely presented earlier than for rural area vegetation. Across the cities we investigated the extent UI gradient was prevalent as a threshold (33.2% ± 2.3%) of surface temperature to SOS advance enhancement and offset. At low urbanization enhanced surface temperature on SOS advances, while at high urbanization offset surface temperature on SOS advances. Overall, UI demonstrated a nonlinear relationship with SOS. The results of this study suggest that there may be thresholds of impact on vegetation SOS in future global climate and environment change processes, where opposite effects can occur below and above thresholds.

Introduction

Vegetation phenology serves as a significant indicator of vegetation dynamics (Shen *et al.* 2018) and is highly sensitive to the impacts of climate change (Zhou *et al.* 2016; Dang *et al.* 2023a). Global warming has the potential to advance the timing of spring phenology (Körner and Basler 2010; Fu *et al.* 2015). Changes in vegetation phenology have implications for the exchange of carbon, water, and energy between the terrestrial biosphere and the atmosphere (Keenan *et al.* 2014; Richardson *et al.* 2013; Piao *et al.* 2008). Because of the association of urbanization with increasing temperature (Zhang *et al.* 2009) and CO_2 concentration, urban climate conditions are considered to be similar to those under future global warming, making urban environments a natural laboratory for simulating the effects of future climate change on phenology (Wang *et al.* 2019; Yuan *et al.* 2020). Therefore, in-depth studies of urban vegetation phenology changes provide insight into future global climate change, carbon cycle, water cycle, energy cycle, and biodiversity.

Previous studies have often compared urban-rural factors affecting phenology (Zhou *et al.* 2016; Jia *et al.* 2021; Li *et al.* 2016; Meng *et al.* 2020), suggesting that urban-rural phenology differences correlate with urban-rural surface temperatures (Yuan *et al.* 2020; Zhang *et al.* 2004; Shao *et al.* 2021). Studies have investigated the different responses of vegetation phenology to urbanization-induced factors such as surface temperature, CO_2 concentration, precipitation, and urban size (Li *et al.* 2016; Qiu *et al.* 2020; Wang *et al.* 2019; Zhang *et al.* 2022b). However, the pattern of spring vegetation phenology response to urbanization gradients has not been assessed regionally. In addition, urbanization does not only increase surface temperature, but also leads to significant changes in other environmental factors (e.g., CO_2, population density, and nighttime lighting). Studies have shown that both temperature and CO_2 concentration are major factors in the advancement of photosynthetic phenology in spring (Wang *et al.* 2019). Moreover, urbanization and climate change jointly shift land surface phenology in large cities (Qiu *et al.* 2020). Therefore, the impact of urbanization on vegetation phenology is the result of a joint action of multiple factors. It is very important to separate the direct and indirect impacts of urbanization on urban vegetation phenology.

Badgley *et al.* (2017) proposed a new vegetation index, the near-infrared reflectance of vegetation (NIR_V), which was the product of the near-infrared band reflectance (NIR) and the normalized difference vegetation index (NDVI) (i.e., $NIR_V = NDVI \times NIR$). NIR_V has a good theoretical basis, eliminates most of the mixed image element problems, and is insensitive to background contamination (Badgley *et al.* 2017). Meanwhile, studies have shown that NIR_V is better than NDVI and enhance vegetation index (EVI) in estimating phenological metrics and in revealing the effects of vegetation phenology on the carbon cycle (Zhang *et al.* 2022a). However, NIR_V has not been used to explore the response of vegetation phenology to urbanization.

To quantitatively assess the impact of urbanization on vegetation phenology, we modified the conceptual framework of the impact of urbanization on vegetation productivity (Zhao *et al.* 2016; Zhuang *et al.* 2022). We propose the following theoretical framework (Figure 2) and give several necessary definitions. Numerous efforts that use the greenness vegetation indices and NIR_V have shown that SOS was advanced in urban areas (Wang *et al.* 2019; Li *et al.* 2016; Meng *et al.* 2020). The total actual impact of urbanization on SOS is the change in SOS after urbanization, including indirect impact and direct impact. Cities such as the cities in Minnesota (Yuan and Bauer 2007), Indianapolis (Lu and Weng 2006), Beijing (Xiao *et al.* 2007) and Shanghai (Li *et al.* 2011) have shown a linear positive correlation between surface temperature and impervious surface cover. Moreover, the negative correlation between start of season (SOS) and temperature is linear. Ideally, a negative correlation between SOS and urbanization intensity (UI) should be linear. Therefore, the direct effect refers to the advancement of SOS due to changes in surface temperature caused by the UI. Post-urbanization environments can alter vegetation phenology (e.g., germination and defoliation), and this effect is indirect. Indirect effects refer to the changes in SOS caused by environmental factors (e.g., CO_2 concentration, population density, and nighttime lighting) as a result of urbanization.

In this study, we used NIR_V extraction of SOS and Moderate Resolution Imaging Spectroradiometer (MODIS) phenology products to explore patterns of SOS relationship to UI in the Northern Hemisphere. The SOS of NIR_V was extracted using two widely used inflection point detection and threshold methods. Meanwhile, the developed conceptual framework was used to quantify the direct and

Chaoya Dang, Zhenfeng Shao, Gui Cheng, and Jiaxin Qian are with the State Key Laboratory Information Engineering Survey Mapping and Remote Sensing, Wuhan University, Wuhan 430079, China (shaozhenfeng@whu.edu.cn).

Xiao Huang is with the Department of Geosciences, University of Arkansas, Fayetteville, Arkansas 72701.

Corresponding author: Zhenfeng Shao (shaozhenfeng@whu.edu.cn)

Contributed by John Rogan, February 3, 2023 (sent for review June 6, 2023; reviewed by Dexter Locke, Alper Yilmaz).

Photogrammetric Engineering & Remote Sensing
Vol. 89, No. 10, October 2023, pp. 639–651.
0099-1112/22/639–651

doi: 10.14358/PERS.23-00008R2

PEER-REVIEWED CONTENT
IS ONLY AVAILABLE TO
ASPRS MEMBERS AND SUBSCRIBERS

FOR MORE INFORMATION VISIT
MY.ASPRS.ORG

PEER-REVIEWED CONTENT
IS ONLY AVAILABLE TO
ASPRS MEMBERS AND SUBSCRIBERS

FOR MORE INFORMATION VISIT
MY.ASPRS.ORG

PEER-REVIEWED CONTENT
IS ONLY AVAILABLE TO
ASPRS MEMBERS AND SUBSCRIBERS

FOR MORE INFORMATION VISIT
MY.ASPRS.ORG

**PEER-REVIEWED CONTENT
IS ONLY AVAILABLE TO
ASPRS MEMBERS AND SUBSCRIBERS**

**FOR MORE INFORMATION VISIT
MY.ASPRS.ORG**

PEER-REVIEWED CONTENT
IS ONLY AVAILABLE TO
ASPRS MEMBERS AND SUBSCRIBERS

FOR MORE INFORMATION VISIT
MY.ASPRS.ORG

PEER-REVIEWED CONTENT IS ONLY AVAILABLE TO ASPRS MEMBERS AND SUBSCRIBERS

FOR MORE INFORMATION VISIT MY.ASPRS.ORG

PEER-REVIEWED CONTENT
IS ONLY AVAILABLE TO
ASPRS MEMBERS AND SUBSCRIBERS

FOR MORE INFORMATION VISIT
MY.ASPRS.ORG

PEER-REVIEWED CONTENT
IS ONLY AVAILABLE TO
ASPRS MEMBERS AND SUBSCRIBERS

FOR MORE INFORMATION VISIT
MY.ASPRS.ORG

PEER-REVIEWED CONTENT
IS ONLY AVAILABLE TO
ASPRS MEMBERS AND SUBSCRIBERS

FOR MORE INFORMATION VISIT
MY.ASPRS.ORG

PEER-REVIEWED CONTENT
IS ONLY AVAILABLE TO
ASPRS MEMBERS AND SUBSCRIBERS

FOR MORE INFORMATION VISIT
MY.ASPRS.ORG

PEER-REVIEWED CONTENT
IS ONLY AVAILABLE TO
ASPRS MEMBERS AND SUBSCRIBERS

FOR MORE INFORMATION VISIT
MY.ASPRS.ORG

WHO'S WHO IN ASPRS

Founded in 1934, the American Society for Photogrammetry and Remote Sensing (ASPRS) is a scientific association serving thousands of professional members around the world. Our mission is to advance knowledge and improve understanding of mapping sciences to promote the responsible applications of photogrammetry, remote sensing, geographic information systems (GIS) and supporting technologies.

BOARD OF DIRECTORS

BOARD OFFICERS

President
Lorraine B. Amenda, PLS, CP
Towill, Inc

President-Elect
Bandana Kar
Oak Ridge National Lab

Vice President
Amr Abd-Elrahman
University of Florida

Past President
Christopher Parrish, Ph.D
Oregon State University

Treasurer
John McCombs
NOAA

Secretary
Harold Rempel
ESP Associates, Inc.

COUNCIL OFFICERS

ASPRS has six councils. To learn more, visit https://www.asprs.org/Councils.html.

Sustaining Members Council
Chair: Ryan Bowe
Deputy Chair: Melissa Martin

Technical Division Directors Council
Chair: Hope Morgan
Deputy Chair: Tao Liu

Early-Career Professionals Council
Chair: Youssef Kaddoura
Deputy Chair: : Greg Stamnes

Region Officers Council
Chair: Demetrio Zourarakis
Deputy Chair: Cody Condron

Student Advisory Council
Chair: Oscar Duran
Deputy Chair: Ali Alruzuq

TECHNICAL DIVISION OFFICERS

ASPRS has seven professional divisions. To learn more, visit https://www.asprs.org/Divisions.html.

Geographic Information Systems Division
Director: Denise Theunissen
Assistant Director: Jin Lee

Lidar Division
Director: Ajit Sampath
Assistant Director: Mat Bethel

Photogrammetric Applications Division
Director: Ben Wilkinson
Assistant Director: Hank Theiss

Primary Data Acquisition Division
Director: Srini Dharmapuri
Assistant Director: Ravi Soneja

Professional Practice Division
Director: Hope Morgan
Assistant Director: Christian Stallings

Remote Sensing Applications Division
Director: Tao Liu
Assistant Director: Indu Jeyachandran

Unmanned Autonomous Systems (UAS)
Director: Jacob Lopez
Assistant Director: Bahram Salehi

REGION PRESIDENTS

ASPRS has 13 regions to serve the United States. To learn more, visit https://www.asprs.org/regions.html.

Alaska Region
Dave Parret

Cascadia Region
Jimmy Schulz

Eastern Great Lakes Region
Craig Fry

Florida Region
Matt LaLuzerne

Gulf South
Stuart Babin

Heartland Region
Whit Lynn

Mid-South Region
David Hughes

North Atlantic Region
Kurt Lutz

Northeast Region

Pacific Southwest Region
Omar Mora

Potomac Region
Jason Brown

Rocky Mountain Region
Melissa Martin

Western Great Lakes Region
Adam Smith

PUBLISHING OPEN-ACCESS IN *PE&RS* IS NOW EASIER!

ASPRS is changing the subscription model of our monthly journal, *PE&RS*. ASPRS is waiving open-access fees for primary authors from subscribing institutions. Additionally, primary authors who are Individual Members of ASPRS will be able to publish one open-access article per year at no cost and will receive a 50% discount on open-access fees for additional articles.

- **Open Access matters!** By providing unrestricted access to research we can advance the geospatial industry and provide research that is available to everyone.
- **Institutions and authors receive more recognition!** Giving permission to everyone to read, share, reuse the research without asking for permission, as long as the author is credited.
- **Reputation matters!** Known for its high standards, *PE&RS* is the industry leading peer-review journal. Adding open access increases authors' visibility and reputation for quality research.
- **Fostering the geospatial industry!** Open access allows for sharing without restriction. Research is freely available to everyone without an embargo period.

Under the previous subscription model, authors and institutions paid $1500 or more in open-access fees per article. This will represent a significant cost savings. Open-access publications benefit authors through greater visibility of their work and conformance with open science mandates of funding agencies.

Subscriptions asprs.org/subscribe
Membership asprs.org/membership

asprs THE IMAGING & GEOSPATIAL INFORMATION SOCIETY

SUSTAININGMEMBERS

ACI USA Inc.
Weston, Florida
https://acicorporation.com/
Member Since: 2/2018

Aerial Services, Inc.
Cedar Falls, Iowa
www.AerialServicesInc.com
Member Since: 5/2001

Airworks Solutions Inc.
Boston, Massachusetts
Member Since: 5/2022

Applanix
Richmond Hill, Ontario, Canada
http://www.applanix.com
Member Since: 7/1997

Ayres Associates
Madison, Wisconsin
www.AyresAssociates.com
Member Since: 1/1953

Cardinal Systems, LLC
Flagler Beach, Florida
www.cardinalsystems.net
Member Since: 1/2001

Dewberry
Fairfax, Virginia
www.dewberry.com
Member Since: 1/1985

Esri
Redlands, California
www.esri.com
Member Since: 1/1987

GeoCue Group
Madison, Alabama
http://www.geocue.com
Member Since: 10/2003

Geographic Imperatives LLC
Centennial, Colorado
Member Since: 12/2020

GPI Geospatial Inc.
Orlando, Florida
www.aca-net.com
Member Since: 1/1994

Halff Associates, Inc.
Richardson, Texas
www.halff.com
Member Since: 8/2021

Keystone Aerial Surveys, Inc.
Philadelphia, Pennsylvania
www.kasurveys.com
Member Since: 1/1985

Kucera International
Willoughby, Ohio
www.kucerainternational.com
Member Since: 1/1992

L3Harris Technologies
Broomfield, Colorado
www.l3harris.com
Member Since: 6/2008

Merrick & Company
Greenwood Village, Colorado
www.merrick.com
Member Since: 4/1995

Miller Creek Associates
SeaTac Washington
www.mcamaps.com
Member Since: 12/2014

Nearmap
South Jordan, Utah
www.nearmap.com
Member Since: 6/2023

NV5 Geospatial
Sheboygan Falls, Wisconsin
www.quantumspatial.com
Member Since: 1/1974

Pickett and Associates, Inc.
Bartow, Florida
www.pickettusa.com
Member Since: 4/2007

PixElement
Belmont, Michigan
https://pixelement.com
Member Since: 2/2017

Riegl USA, Inc.
Orlando, Florida
www.rieglusa.com
Member Since: 11/2004

Sanborn Map Company
Colorado Springs, Colorado
www.sanborn.com
Member Since: 10/1984

Surdex Corporation
Chesterfield, Missouri
www.surdex.com
Member Since: 12/2011

Surveying And Mapping, LLC (SAM)
Austin, Texas
www.sam.biz
Member Since: 12/2005

T3 Global Strategies, Inc.
Bridgeville, Pennsylvania
https://t3gs.com/
Member Since: 6/2020

Towill, Inc.
San Francisco, California
www.towill.com
Member Since: 1/1952

Woolpert LLP
Dayton, Ohio
www.woolpert.com
Member Since: 1/1985

SUSTAININGMEMBER**BENEFITS**

Membership

- ✓ Provides a means for dissemination of new information
- ✓ Encourages an exchange of ideas and communication
- ✓ Offers prime exposure for companies

Benefits of an ASPRS Membership

- Complimentary and discounted Employee Membership*
- E-mail blast to full ASPRS membership*
- Professional Certification Application fee discount for any employee
- Member price for ASPRS publications
- Discount on group registration to ASPRS virtual conferences
- Sustaining Member company listing in ASPRS directory/website
- Hot link to company website from Sustaining Member company listing page on ASPRS website
- Press Release Priority Listing in *PE&RS* Industry News
- Priority publishing of Highlight Articles in *PE&RS* plus, 20% discount off cover fee
- Discount on *PE&RS* advertising
- Exhibit discounts at ASPRS sponsored conferences (exception ASPRS/ILMF)
- Free training webinar registrations per year*
- Discount on additional training webinar registrations for employees
- Discount for each new SMC member brought on board (Discount for first year only)

*quantity depends on membership level